DEVELOPMENT OF A HIGH TEMPORAL RESOLUTION ELECTRONIC SUN JOURNAL FOR MONITORING SUN EXPOSURE PATTERNS

A thesis submitted by

Raja Salem Elrahoumi

BSc. (Physics)

For the award of

Master of Science (Research)

2018

Abstract

Excessive exposure to UV radiation can significantly damage human health. Exposure to UV radiation causes acute effects and long-term effects. Examples of acute effects are sunburn (erythema), immunosuppression and photokeratitis. Long-term effects include melanoma and other skin cancers and ocular disease such as pterygium and cataracts. Measuring personal solar UV exposure and determining sun exposure patterns is important for public health, as more knowledge is needed to define the causes of diseases related to sun exposure. Many studies have employed paper-based sun diaries (journals) or employ expensive electronic dosimeters (which limit the size of the sample population) to estimate periods of exposure.

A cost-effective personal electronic sun journal (ESJ) is developed in this project, which introduces a novel methodology for sensing outdoor exposure patterns. This methodology has not been previously employed for personal solar exposure monitoring. The ESJ was built from a UV infrared photodiode, which was tested in this project to determine if it can be utilised in a personal ESJ, for characterising personal UV exposure patterns. The development of the ESJ was undertaken by testing a group of photodiodes for their physical response. These photodiodes were chosen due to their low cost, their sensitivity to infrared radiation and their cosine response as listed by their manufacturer. The photodiode with the best cosine response was selected to be one of the ESJ circuit elements. The other elements are a 20 kΩ resistor, a 3 V battery and a Tinytag TK-4703 voltage data logger. Preliminary environmental tests were conducted on the ESJ to ensure that it operated correctly and is sensitive to the environment. After the preliminary tests, other tests were performed, including the cosine response test, temperature stability test and sky view test. Environmental characterisation tests were then performed by placing the ESJ in different types of static environments. The ESJ has been used in conjunction with ambient UV meters to estimate the erythemally effective UV exposure. Five individual walking tests, or field trials, were performed, with each trial involving the

researcher holding a wooden board with the ESJ and PMA2100 meter and the researcher walking around and through different types of environments with a variety of shade protection. Preliminary environmental test results showed that the ESJ is sensitive to the environment. The temperature stability test showed that the ESJ can be employed in normal summer and winter temperatures. The sky view tests showed that a decrease in sky view leads to an increase in output voltage. Environmental characterisation tests demonstrated the ability of the ESJ to classify the type of environment typically occupied by users. In terms of the characteristics of each tested environment, there was increased output voltage by the ESJ with increasing shade density (reduced sky view). Results of individual walking tests confirmed the ability of ESJ to detect individual exposure patterns.

The greater detail thereby obtained regarding behavioural exposure patterns cannot be obtained by using paper-based sun diaries. Based on the results of this research, the ESJ could replace paper-based sun journals. The latter depend on self-reported volunteer recall, which is subjective and possibly marred by public social desirability bias. The ESJ data offers greater objectivity and could complement existing exposure monitoring in UV research studies for estimating periods of exposure patterns. Using the ESJ further improves the accuracy of long-term epidemiological cumulative exposure studies as high sampling rates can be obtained using this more affordable tool.

Certification of Thesis

This Thesis is entirely the work of Raja Elrahoumi except where otherwise acknowledged. The work is original and has not previously been submitted for any other award, except where acknowledged.

Principal Supervisor: Professor Alfio Parisi

Associate Supervisor: Dr Nathan Downs

Associate Supervisor: Dr Harry Butler

Student and supervisors signatures of endorsement are held at the University.

ACKNOWLEDGMENTS

I would like to expresse my special thanks and respect to my supervisores Dr Nathan Downs, Professor Alfio Parisi and Dr Harry Butler for their advice, patience and guidence during this research.

I would like also to express my very profound gratitude to my parents and my husband for continued support throughout this degree.

I would like to thank the Australian Commonwealth Government contribution through the Research Training Program (RTP) Fees Offset scheme during my research.

Contents

List of Figures

List of Tables

1 Chapter 1: Literature Review

1.1 Introduction

Sunlight is a continuous spectrum of electromagnetic radiation. The incident energy per wavelength of the electromagnetic spectrum is the solar spectral irradiance. Solar spectral irradiance is measured in units of *watts per metre squared per nanometer* (W m^{-2} nm^{-1}). Spectral irradiance is dependent upon the temperature of the emitting source. Peak spectral irradiance approaches shorter wavelengths with increasing temperature. The surface temperature of the Sun is approximately 6000 K, with the peak solar irradiance occurring in the visible waveband of the electromagnetic spectrum. The solar spectrum is distributed over a wide range of wavelengths, of which three wavebands contribute to most of the available radiation (Narayanan et al. 2010). These include the ultraviolet (UV) waveband, consisting of the wavelengths shorter than 400 nm; the infrared waveband, consisting of wavelengths longer than 700 nm; and the visible waveband consisting of wavelengths between 400 and 700 nm (Figure 1-1). The shorter wavelengths in the visible waveband (400 nm) correspond to violet light and the longer wavelengths in the visible waveband correspond to red light (Parisi 2005). The three wavebands together are referred to as optical radiation. The waveband that has the most significant impact on human health is ultraviolet radiation (UV) (Diffey 2002).

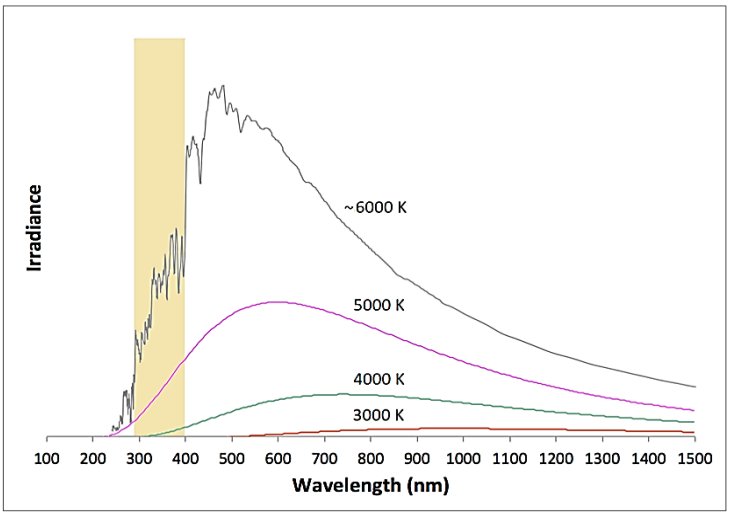

Figure 1-1: Spectral irradiance distribution for objects of different temperatures, including the measured solar spectral irradiance from 240 nm to 1500 nm (Woods et al. 2015). The shaded region represents the UV waveband (Downs et al. 2016).

The range of UV radiation exists between the wavelengths of 100 and 400 nm (IARC 2015). This range is divided further according to the biological effects of the radiation into three regions: Ultraviolet C (UVC), (100–290 nm), Ultraviolet B (UVB), (290–320 nm), and Ultraviolet A (UVA), (320–400 nm) (Hussein 2005). Most of the UV that reaches the Earth's surface is UVA (95%) and a small part is UVB (5%) (Greinert et al. 2015). No UVC radiation reaches the Earth's surface due to absorption by the Earth's atmosphere (Hussein 2005). Figure 1-2 below shows a typical solar UV spectrum and the UVA and UVB wavebands after absorption by the atmosphere (Parisi 2005). As shown in the spectrum, there are some dips due to Fraunhofer absorption lines by elements in the Sun's atmosphere (Parisi 2005). This absorption occurs at wavelengths by elements such as calcium, iron, titanium, aluminium and magnesium (Parisi & Turnbull 2005).

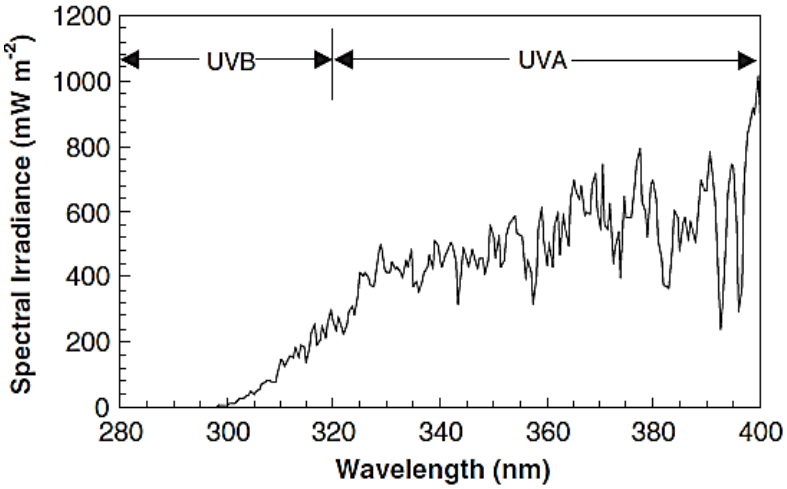

Figure 1-2: Typical solar irradiance from 280 to 400 nm measured in Toowoomba, (Parisi et al 2008).

1.2 The Influence of the Atmosphere

The amount of UV radiation reaching the Earth's surface depends upon many variables, comprised of atmospheric attenuation by gases including ozone, reflection and absorption by cloud and particulate matter, and the solar elevation, which influences the optical path of the incident radiation.

1.2.1 Diffuse, direct and global radiation

The received solar irradiance at the Earth's surface is a sum of *direct* solar radiation and *diffuse* radiation (Kerr 2005). Direct radiation is the radiation incident directly from the solar disc. Diffuse, or skylight, radiation is caused by the processes of scattering, reflection or absorption by clouds, air, dust and atmospheric gases (Ambas & Baltas 2014). The diffuse fraction is a significant component of the total incident radiation on the Earth's surface. Diffuse radiation consists of between 17% and 59% of the total available solar radiation and increases when the sun is lower in the sky and the optical path of the radiation is greatest (Parisi et al. 2001). Global radiation is the sum of both direct and diffuse

radiation components.

1.2.2 Absorption by atmospheric gases

UVB radiation is absorbed by atmospheric ozone, while the absorption due to ozone in the UVA waveband is very low, and where UVA absorption drops significantly before 320 nm (Parisi & Kimlin 2005a; Madronich et al. 1998). Ozone moderates the absorption of UV radiation of wavelengths up to approximately 320 nm by the dissociation of ozone (O_3) into oxygen (O_2) and a single free oxygen (O) atom (Chapman 1930, cited in Diffey 1991). UVB radiation is also absorbed by other atmospheric gases, including sulfur dioxide (SO_2) and nitrogen dioxide (NO_2) (Kerr & Fioletov 2008; Kerr 2005). Stratospheric ozone is a considerable absorber, decreasing the received erythemally effective (sunburn (see section 1.3.1.1)) radiation on the Earth's surface to less than 3% (Kerr & Fioletov 2008). For more than three decades, ozone depletion has been the major cause of the increase in UVB radiation at the Earth's surface (Kerr 2005). UVB increases, particularly in the Southern hemisphere, are caused by depleted ozone concentration and seasonal variations over the Antarctic (Kerr 2005).

1.2.3 The effect of cloud

Clouds play an important role in determining the amount of UV radiation reaching the Earth's Surface. Like any other optical medium, clouds may reflect, refract, absorb and scatter incident radiation across the solar spectrum (IRAC 2012). The primary method of cloud attenuation is scattering (Diffey 2002). As the wavelength of UVA and UVB is smaller than the radii of cloud droplets (which are from 1 to 30 μm), the attenuation across the wavelength of UVA and UVB spectrum is constant and not dependent on wavelength. In general, UV radiation received on the Earth's surface is attenuated by clouds (Bais et al.

2015). The attenuation of infrared radiation by clouds is much more than the attenuation of UV radiation by clouds, as water in clouds reduce infrared radiation more than UV radiation (Diffey 2002). The attenuation of UV radiation depends on the total amount of cloud cover (sky coverage), cloud thickness or depth and the cloud type (total water and ice content) (Bais et al. 2015). It has been reported that UV radiation can be attenuated to 90% under heavy cloud cover conditions (WHO 1994). For overcast skies, surface UV radiation is always less than that observed in clear conditions (Kerr 2005). Where there is broken cloud, direct UV radiation is attenuated significantly but if the sun is not obscured then the attenuation can be low (Kerr 2005) and enhancement greater than that observed under clear conditions may occur. Figure 1-3 below shows that clouds, generally, reduce UV radiation. Enhancement above the level of clear sky irradiance is highlighted in red in the figure below.

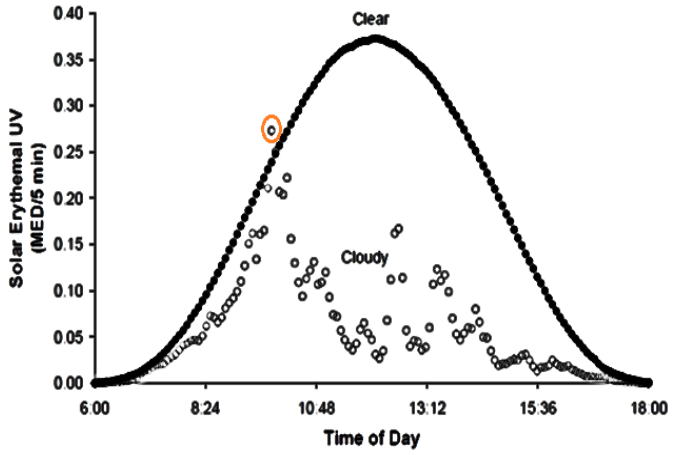

Figure 1-3: The influence of a cloudy sky on global UV irradiance compared to a clear sky (Turnbull 2005).

In addition to the role cloud has in attenuating UV radiation, cloud cover may enhance the

UV irradiance above the irradiance expected under cloud-free conditions (IRAC 2012). This enhancement in the UV radiation is independent of wavelength in the wavelength range longer than 306 nm and wavelength dependent for wavelengths of less than 306 nm (Sabburg et al. 2003). Sabburg and Wong (2000) reported that 86% of UV enhancements due to cloud cover occurred under hazy, cirrus skies.

1.2.4 Aerosols – dust and particulate matter

Atmospheric aerosols have a significant role in attenuating the UV irradiance reaching the Earth's surface. Aerosol properties of scattering and absorption depend strongly on wavelength, relative humidity and the chemical properties of the aerosol particles (Kikas 2001; Kerr & Fioletov 2008). The aerosol scattering process depends on the wavelength and angular distribution of incident UV radiation and depends on the size, and shape of the aerosol particles (Kerr & Fioletov 2008).

Aerosols are particles suspended in the atmosphere and originate from different sources (natural or manufactured). The natural sources include deserts, forest fires and volcanoes. Natural aerosols also include dust and suspended sea salt. The manufactured sources of aerosol consist of emissions from factories, power plants, biomass burning, car exhausts, and aircraft emissions. Manufactured aerosols include soot, sulfate, and organic particles (Bais et al. 2015; Kerr & Fioletov 2008).

The influence of aerosols on UV radiation is often expressed by the Aerosol Optical Depth (AOD). The AOD in the UV waveband (λ) is determined by the natural logarithm of the ratio of direct solar radiation including aerosols to that without aerosols in the path of the direct UV radiation divided by the relative path length through the atmosphere, where the

relative path length is defined by $\sec\theta$ and θ is the solar zenith angle (see section 1.2.5) (Kerr & Fioletov 2008).

$$AOD(\lambda) = \frac{\ln\frac{Direct}{Direct\ clear}}{Sec\ \theta} \qquad (1.1)$$

Scattering and absorption affects the AOD; however, absorption is the most effective process in attenuating UV radiation at the Earth's surface (Bais et al. 2015). The AOD is wavelength dependent, since different aerosols absorb radiation at different wavelengths (Kerr & Fioletov 2008).

1.2.5 Solar elevation

Solar elevation above the horizon has a significant influence in varying the received spectrum and intensity of UV irradiance on the Earth's surface, as this directly influences the optical path length (Diffey 2002). Solar elevation is typically expressed in terms of the solar zenith angle (SZA), which is the angle between the local vertical and the direction of the solar disc. The SZA depends on the time of the day, the day of the year, and the latitude and longitude of the location (Stamnes & Stamnes 2008; Diffey 2002). Increasing SZA leads to a decrease in incident surface UV radiation on the horizontal surface. This decrease occurs for two reasons. The first is that the incident UV radiation measured on a horizontal plane at the ground surface $UV(\theta)$ will be proportional to the cosine of the SZA as follows:

$$UV(\theta) = UV_D \cos(\theta) \qquad (1.2)$$

where θ is the SZA and UV_D is the direct UV radiation (Parisi 2005). The second reason for the decrease with increasing SZA is that the relative path length of direct radiation passing through the atmosphere will increase and this leads to an increase in absorption

and scattering processes by atmospheric gases and aerosols through the atmosphere (Kerr & Fioletov 2008).

1.3 UV Radiation and Health

Excessive exposure to UV radiation can significantly damage human health (Turner & Parisi 2009). Exposure to UV radiation causes acute effects such as sunburn (erythema), immunosuppression and photokeratitis (inflammation of the cornea) (Young 2006). Long-term effects include melanomas and keratinocyte skin cancer (Turner & Parisi 2009; Downs et al. 2009) and ocular diseases such as pterygium and cataracts (AAP 2011).

1.3.1 Harmful effects of UV radiation on human health

1.3.1.1 Sunburn

The most common acute effect of too much exposure to UV is erythema or sunburn (AAP 2011). Erythema is redness in the human skin that appears after too much exposure to sunlight. It occurs due to enhancement in dermal blood flow (Diffey 1998). On an average summer weekend, about 8% of children, 14% of adults and 24% of teenagers are suffering from sunburn in Australia (CCA 2015a). There are several biological factors that affect sunburn, such as skin hydration, skin type (colour and thickness), age and anatomical site. The severity of any sunburn depends on the intensity and total exposure to incident UV. Thus, the absorbed biologically effective dose is influenced by physical factors that affect SZA, including local latitude and time of the day. Local altitude, which influences the total absorption of UV and environmental reflection (surface albedo) also contribute to the severity and body surface area affected by sunburn (Honigsmann 2002).

1.3.1.2 Skin cancer

Lifetime exposure to solar UV radiation and a history of sunburn is the essential cause of skin cancer incidence (Greinert et al. 2015). UV exposure can damage DNA, leading to genetic mutations (Narayanan et al. 2010). Exposure to naturally occurring sunlight causes most of the skin cancer in Australia, where 80% of newly diagnosed cancers are skin cancer cases (CCA 2015a). Australia spends significant amounts in the health system due to skin cancer, with estimates exceeding $300 million per annum (CCA & ACD 2009, p. 6). This shows the importance of studying the outdoor exposure times and patterns of personal behaviour to determine what is required to avoid significant risk factors for the development of skin cancer.

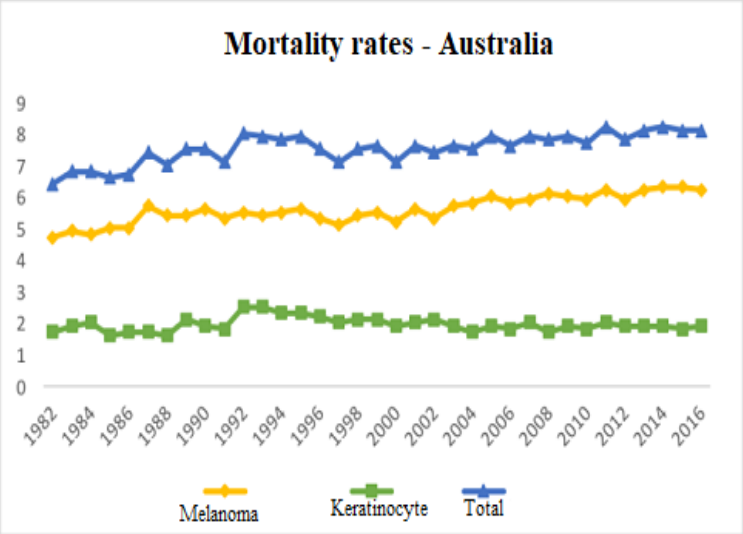

Figure 1-4: Mortality rates in Australia due to keratinocyte skin cancer (KSC) and melanoma skin cancer (CCA 2016).

There are two main types of skin cancer: melanoma and keratinocyte skin cancer (KSC). KSC may be broadly divided into two categories, basal cell carcinomas (BCC) and

squamous cell carcinomas (SCC) (Hussein 2005). Skin colour, or type, plays an important role in melanoma incidence (Leiter & Garbe 2008). Melanoma cancer rates are highest in fair skin types, with other risk factors including the total number of nevi (or moles) on the body surface (Green et al. 1989).

Melanoma is considered the sixth most common cause of cancer mortality in Australian men and tenth in Australian women (CCA 2015a). According to the Cancer Council Australia (2016 – Figure 1.4), total reported skin cancer rate (blue) is steadily rising. Between Melanoma and Keratinocyte skin cancer, melanoma mortality is still rising while keratinocyte skin cancer mortality rates are low and steady. The number of deaths in Australia attributed to melanoma in 2014 were 1400 (Melanoma Institute Australia 2018). In 2013, the Australian Bureau of Statics (ABS) reported that the number of deaths attributed to melanoma was 1617 (CCA 2015b).

While mortality for KSC cancer is low, incidence in fair skinned populations is much higher than that of melanoma (AAP 2011). Both types of KSC, but especially SCC, tend to occur on sun exposed regions of the body (Narayanan et al. 2010). KSC is a very common cancer in Australia. KSC deaths reported by the Australian Bureau of Statics totalled 592 in 2013 (CCA 2015b).

1.3.1.3 Eye disorders

Human eye exposure to solar UV radiation causes damage to its structure (Jaggernath et al. 2013). There are many factors that affect human eye exposure to UV radiation; these include physical factors that affect the available ambient radiation and the anatomy of the face (Wang et al. 2014). Excessive UVR exposure may result in acute and chronic effects

on the human eye (Jaggernath et al. 2013). Common acute effects resulting from excessive eye exposure to UVR include photokeratitis (snow blindness) and photoconjunctivitis. Photokeratitis and photoconjunctivitis are caused by exposure of the corneal surface layer to UVC and UVB radiation (Young 2006). This may be caused by welding flash or exposure to intense solar UV. Other adverse effects of eye exposure to UV radiation comprise climatic droplet keratopathy, uveal melanoma, pterygium, ocular surface squamous neoplasia, and cataracts (Majdi et al. 2014). Exposure to UV radiation is also related strongly to eyelid cancers such SCC and BCC (Yam & Kwok 2013).

1.3.1.4 Immunosuppression

Long term exposure to UV radiation (especially UVB) leads to suppression of the immune system. Immunosuppression effects also have an important role in skin cancer development (Damian et al. 2011; Whiteman & Neale 2004). Limited exposure to solar UV radiation may lead to an increase in the hazard of bacterial, viral and parasitic infections, and too much exposure to UV radiation can reduce the influence of vaccination (Wright et al. 2017).

1.3.2 Beneficial effects of UV radiation

1.3.2.1 Vitamin D

Exposure to UV radiation plays a major role in inducing vitamin D production in human skin. This vitamin is very significant for human health, because it is required for calcium absorption from food (De Gracuijl 2000). Thus, vitamin D has a major role in maintaining bones and muscle health (CCA 2015b). Up to 90% of the production of vitamin D occurs in the skin when it is exposed to UVB radiation (Locus & Ponsonby 2002) through a chain

of biochemical processes (CCA 2015b). Another source of vitamin D is obtained through diet which may include foods fortified with vitamin D and oily fish (van der Gaag & Brekhoff 2014).

Vitamin D and calcium intake benefit human health by preventing rickets, osteomalacia and hip fractures, especially in the elderly (Grant 2007). Decreasing Vitamin D levels in the blood may also be associated with several diseases, such as breast, prostate, and colorectal cancers, and multiple sclerosis (Turnbull & Parisi 2010; (Acherio et al. 2010), so maintaining a healthy vitamin D level may also contribute toward decreasing the risk of cancer occurrence (Grant 2007).

The adequate level of vitamin D for the human body is likely to be 50 nmol/L in Australia at the end of winter and (60–70 nmol/L) at the end of summer (Osteoporosis Australia 2014). There are suggestions that the required level of Vitamin D for bone health is more than 75 nmol/L (CCA 2015b). It has been published by the Australian and New Zealand Bone and Mineral Society, Osteoporosis Australia, Australian College of Dermatologists, Cancer Council Australia and Endocrine Society, that a healthy vitamin D level can be maintained by exposure of sufficient skin surface area to sunlight for as little as five minutes in periods when UV at its peak during the day in summer, and by exposure to 2 to 3 hours per week in winter (PS 2006; Downs et al. 2009).

Vitamin D and diseases related to vitamin D insufficiency correlate with latitude, indicating the importance of exposure to UV radiation in maintaining human health and preventing various diseases (Ascherio et al. 2010).

1.3.2.2 Mental health

Radiation from the sun has a significant effect on mental health (Juzeniene et al. 2011). Exposure to sunlight can lead to an energy boost and mood enhancement (Sivamani et al. 2009). This occurs during exposure to UV radiation, where the β endorphin produced in the blood reaches the brain to simulate mood elevation and the sensation of relaxation (Juzeniene & Moan 2012).

1.4 Determining Sun Exposure Patterns

1.4.1 Sun diaries

There are many studies employing sun diaries to measure sun exposure (O'Riordan et al. 2008). Traditional sun diaries provide a method of estimating the time people spend exposing themselves to solar UV by using questionnaires or giving them diaries to record their daily activity, indoors or outdoors during a specific period of time (Chodick et al. 2008). Sun exposure activities, behaviour and location are often recorded, and participants may be asked if they are sitting or lying in the sun, whether they are at the beach, or if they are at school or work. Often, the information that can be gathered in a sun diary is limited as study participants may only be required to choose yes or no for each question (Thieden et al. 2004). There are some limitations for personal exposure diaries as people may report exposure patterns that reflect a social desirability bias (people record what they think and feel the researcher or others want as a response, not what they really do) (O'Riordan et al. 2008). In addition to that, sun diaries are not an appropriate method to assess the real time UV radiant exposure for large numbers of participants because holding the diaries may affect their exposure behaviour (Koster et al. 2015).

Sun diaries however, are the main tool employed in sun exposure studies because electronic dosimeters cannot be provided for large numbers of participants due to their expense. Table 1.1 below provides a summary of 26 previous personal UV dosimeter studies together with the type of dosimeter employed in each study and the number of participants.

Table 1-1: PubMed review summary of recent solar dosimetry studies since 2000 showing a low number of studies used electronic dosimeters.

Paper Reference	**The number of participants**	**Dosimeter Type**	**How the time is recorded**	**What they measure**	**Study period**
O'Riordan et al. 2000		Polysulphone dosimeter.	A diary based on recall	UVR exposure	4 days
Temorshuizen et al. 2002	1672 participants		Questionnaire	Sunlight exposure	6 weeks
Thieden et al. 2004	164 volunteers	Electronic dosimeters.	Sun diaries	The annual UV dose and sun exposure behaviour	1 year
Thieden et al. 2005	106 participants	Personal electronic UV dosimeter	Diaries and questionnaire	Time stamped UV doses Sun exposure patterns	4 months
Thieden 2005	340 participants	Electronic dosimeters	Sun diaries	Time stamped UV doses Sun exposure and sunscreen use	119 days
Parisi et al. 2006	6 different outdoor activities (7 different anatomical sites)	Polysulphone film dosimeter and broadband meters	Observation, videos and sun diaries	Personal exposure to UVR	
Thieden et al.2006	19 participants (year) + 28 participants (in winter half year)	Personal electronic UV dosimeter SunSaver	Sun diaries	Time stamped UV doses and sun exposure behaviour	1 year

Wright et al. 2007	345 participants	Electronic dosimeter	Sun diaries	UVR exposure and sun protection practice	1-week period over 12 weeks
Chodick et al.2008	124 participants	Polysulphone dosimeters	Sun diaries	Personal UVR doses and self-recorded time spent outdoor	7 days
Thieden 2008		Electronic dosimeter (Sun Saver)	Sun diaries	Time stamped UVR doses and sun exposure behaviour	346 sun years
O'Riordan et al. 2008	27 participants	Polysulphone dosimeter	A survey and sun habits diary and rirect observation of the sun protection practices	UVR exposure and sun protection practices	4 days
O'Riordan et al 2009	162 lifeguards and 201 parent/child pairs		Survey, sun habits diary and observation of sun protection behaviours	To validate self-reported covering-up practice of pool-goers	4 days
Downs & Parisi 2009	147 participants	Polysulphone film dosimeters		Solar erythemally effective exposure	5 months
Schmalwieser et al. 2010	12 participants	Optoelectronic Personal UV-meters	Digital diaries	Facial solar erythemally effective exposure	6 months
Siani et al. 2011	32 participants	Polysulphone dosimeters		Exposure to ambient UV radiation	
Serrano et al. 2011	10 mountaineers, four tennis players and five runners	VioSpor dosimeters		Quantify UV exposure	From May to July 2010
Serrano et al. 2011	10 participants	VioSpor dosimeters		UVR exposure	3 months

Serrano et al. 2012	3 age groups (7–8, 9–10 and 11–12 years old) and involved 15 schoolchildren.	VioSpor dosimeters		To quantify the exposure to solar ultraviolet erythema exposure during doing activities outside	During July 2008.
Serrano et al.2012	15 participants	VioSpor Dosimeters		Personal exposure to UV erythema radiation	1 month
Petersen et al. 2013	25 participants	Personal electronic UVR dosimeters (SunSaver)	Sun diaries	Sun exposure behaviour and its impact on personal UVR exposure	6 days
Sun et al. 2014	991 participants	Polysulphone dosimeters		Personal UVR exposure	From 2009 to Dec 2010
Sun et al. 2014	1002 participants	Polysulphone dosimeters	Questionnaires, sun diaries and face to face interviews	UVR exposure	10 consecutive days
Bodekeaer et al. 2015	150 participants	Electronic dosimeters	Sun diaries	Personal sun exposure and sun exposure behaviour	3.5 months
Koster et al. 2015		UV electronic dosimeter	Smart phone diaries and questionnaire	To show the feasibility of dosimeters and smartphones as a data collection tool	7 days
King et al. 2016	333 participants	Polysulphone dosimeters	Sun diaries	This study determinant of the amplitude and phase and those of inter-individual variability in seasonal pattern	12 months
Koster et al. 2016	240 participants	Personal electronic UV dosimeter.	Sun diaries	Measurement period and recall effect on sun related behaviour.	Around 7 weeks

1.5 Units of Measurement

The total solar irradiance (TSI) is defined as the total energy of the incident solar radiation received by a unit area of the top layer of the Earth's atmosphere (Nan-bin 2014). The TSI is presented in units of watts per metre squared (Solanki et al. 2013). The surface irradiance is measured following transmission through the atmosphere and includes the UV irradiance measured across the UV spectrum.

1.5.1 Ultraviolet irradiance

Ultraviolet irradiance is the incident power per unit area and is measured in watts per metre squared (W/m^2) (Amar 2014, p. 9). The irradiance incident on a surface over a time period is referred to as the radiant exposure.

1.5.2 Ultraviolet exposure

Ultraviolet exposure is the incident energy on the unit area of the surface measured in joules per square metre (J/m^2). There are two additional units that have been widely employed to measure the biologically effective UV exposure that are weighted with the erythema action spectrum. These units are the MED and SED (see sections 1.4.5 and 1.4.6).

1.5.3 Biologically effective exposures (Action Spectra)

An Action Spectrum is a function that describes the biological effectiveness of an exposure per unit of wavelength (Wainwright 2012, p. 13). Different action spectra have been developed for different biological effects (Wainwright 2012, p. 13), such as the erythema action spectrum as shown in Figure 1-5 (CIE 1987), which have been used commonly to evaluate the influence of UV radiation in human skin (Wong & Parisi 1999). Other

examples of action spectra include one for DNA damage (Caldwell et al. 1983), as shown in Figure 1-6 below, and the action spectrum for biological damage to plants as shown in Figure 1-7.

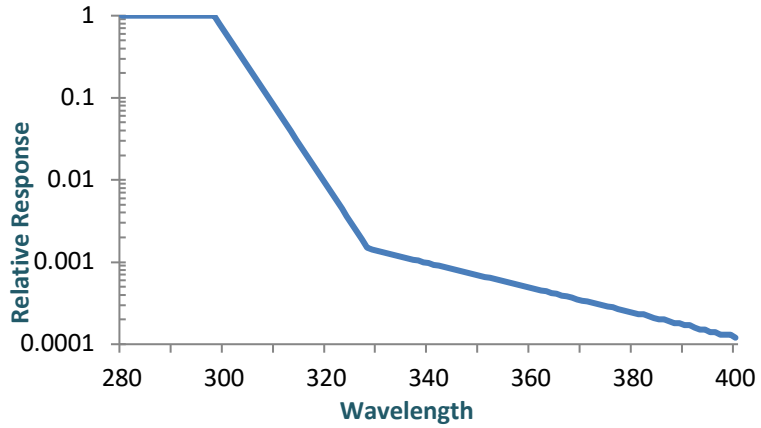

Figure 1-5: The Erythema Action Spectrum (CIE 1987).

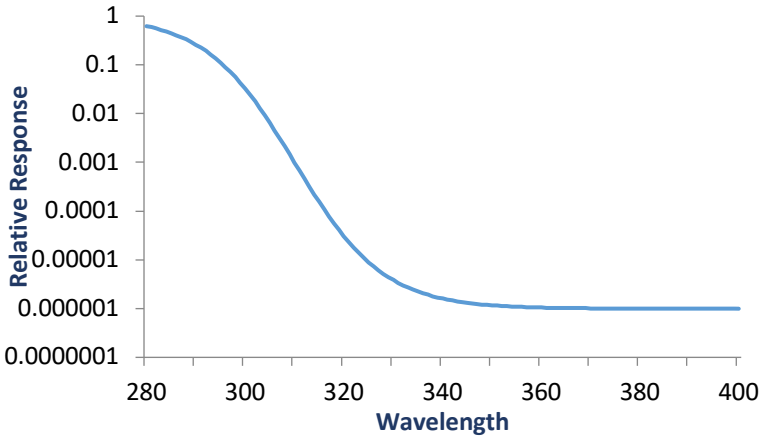

Figure 1-6: The action spectrum of DNA damage (Caldwell et al. 1983).

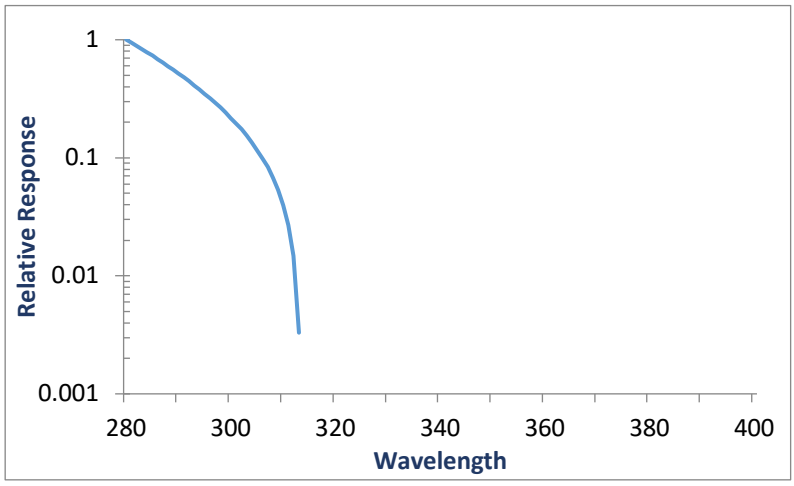

Figure 1-7: The action spectrum of plant damage (Coohill 1989).

The biological damage caused by UV radiation is determined by the equation below for known action spectrum A(λ).

$$UV_{BE} = \int_{290}^{400} S(\lambda)A(\lambda)d\lambda \qquad (1.3)$$

Here S(λ) is the spectral irradiance in units of W/m²/nm and UV_{BE} is the integration over the UV wavelength range from 290 to 400 nm.

Comparative values between 0 and 1 are used to present the effectiveness of the action spectrum (Wainwright 2012, p. 6). The erythema action spectrum is normalised to 1 at the wavelength of 298 nm (Wong & Parisi 1999). In the case of wavelengths longer than 298 nm, the action spectrum value decreases from 10^{-3} to10^{-4} in the UVA (Parisi 2004).

Presenting the action spectra and recognising the biological effectiveness of UV radiation exposure provides a good reason to develop a new electronic device to measure general

sun exposure patterns and the time people spend outside.

1.5.4 Minimal erythema dose (MED)

Individual sensitivity to sunburn is specified by the minimal erythema dose (MED), which is defined as the minimal UV radiation dose that produces minimal redness or perceptible sunburn within 24 hours following exposure to sunlight (Harrison & Young, 2002). The MED depends on skin type and thickness, the concentration of melanin in the epidermis and radiation density (AAP 2011). The MED is utilised as a widespread dose unit in photobiology but, due to variation in skin type, the energy required to produce 1 MED will vary from a minimum dose of approximately 200 J/m^2 for very fair skinned individuals (Young 2006).

1.5.5 Standard erythema dose (SED)

An SED is the standard erythemal dose, which is the equivalent to an erythemal exposure of 100 J/m^2 (Parisi 2005). This unit is independent of skin type.

1.5.6 UV index

The UV index (UVI) is an internationally recognised dimensionless scale used to determine the level of skin damaging UV radiation at the Earth's surface (WHO 2002). The UVI presents values extending from zero upwards. These values are obtained by multiplying the erythemal UV irradiance (W/m^2) by 40 (Parisi 2005). UVI values of 0, 1 or 2 are classified as low, values of 3, 4 or 5 as moderate, values of 6 or 7 as high, values 8, 9 or 10 as very high, and values of 11 or more are considered extreme (WHO 2002).

The UVI is reported in daily forecasts for the public in many countries worldwide (WHO 2018). It is an easily understandable tool used to inform people about the UV level daily.

It is recommended by public health organisations that when the UV index reaches 3 or more, people should protect themselves from exposure to sunlight (WHO 2002).

1.6 Measuring UV Radiation

1.6.1 Measuring environmental radiation

There are various instruments used to measure solar irradiance, depending on the type of irradiance to be measured. For example, direct solar irradiance is measured using a pyrheliometer; global solar irradiance is measured by a pyranometer; and diffuse solar irradiance is measured by a pyranometer equipped with shadow band to shield it from direct solar irradiance (Lysko 2006, p. 10).

These instruments are used for the whole solar spectrum. There are many variants of these instruments which are used to measure solar UV (Wright & Griffith 2015). These instruments include Broadband meters, spectroradiometers and multichannel (moderate and narrow band) radiometers (Di Menno et al. 2002).

1.6.1.1 Broadband meters

The more common radiometers for monitoring solar UV radiation are broadband erythema weighted meters, which are employed to measure the biologically effective erythema-weighted radiation (Leszczynski 2002). The Robertson–Berger (R-B) meter was the first broadband instrument employed to monitor UV radiation (Deluisi et al. 2003). The device contains a phosphor to convert UV radiation to visible light, which is detected by a photodiode (Seidlitz & Krins 2006).

The World Meteorological Organisation reported that broadband meters are a good option

to detect UVB radiation (Cancillo et al. 2005). Examples of instruments include the Yankee Environmental Systems UVB-1, Kipp and Zonen's UV-S-AB-T Solar Light Biometer radiometer, and EKO's MS-212D (Deluisi et al. 2003). Figure 1-8 shows pictures of a Kipp and Zonen broadband UV-radiometer, UV biometer 501 and YES UVB-1. All meter sensors are sealed in a quartz glass, temperature-controlled dome.

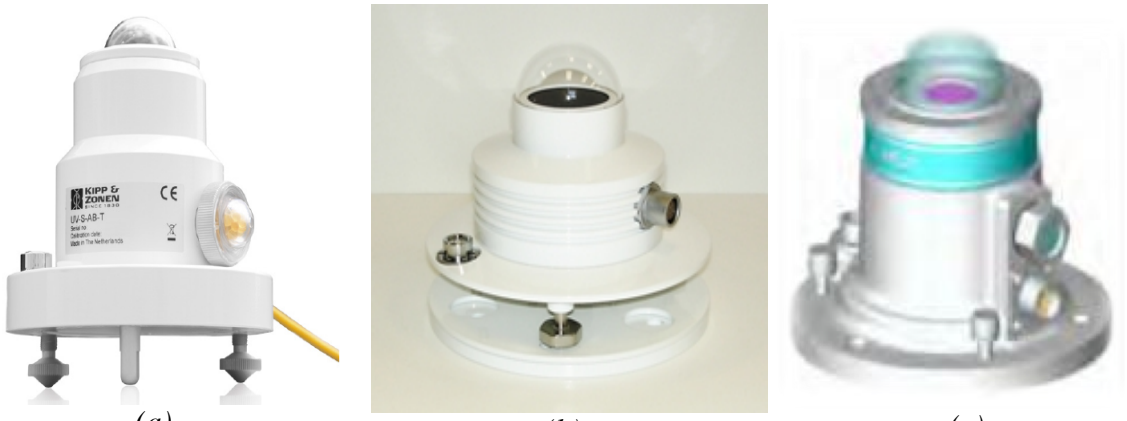

(a) (b) (c)

Figure 1-8: (a) Kipp and Zonen (UV-S-AB-T) broadband UV radiometer (b) UV biometer 501 and (c) YES UVB-1.

The structure and the main parts of each broadband meter differ from each other, but the essential working principles of the instruments are the same. Solar radiation incident on the detector is filtered to prevent visible light and infrared radiation from passing through, allowing just UV radiation entry. A fluorescing phosphor layer converts the UV radiation to visible radiation. This radiation is detected by a photodiode after passing through a green post filter to absorb the remaining UV radiation (Leszczynski 2002). The photodiode current output is converted to voltage by a thermally stable amplifier. The generated electrical output of the broadband UV meter is converted to digital format for electronic logging (Aphalo et al. 2012). Electronic output is frequently calibrated to a UV source

enabling the UV meter to measure solar UV radiation. The broadband meters are easy to use, relatively inexpensive instruments and their measurement is reliable (Cancillo et al. 2005). Moreover, they offer a fast response, good stability, and require low maintenance. These advantages make them common instruments suitable for permanently mounted UV monitoring applications (Aphalo et al. 2012).

The spectral response of the broadband meters should follow the erythema action spectrum (Leszczynski 2002). Figure 1-9 below shows the spectral response of the 501 UV biometer detector; the response is close to the erythema action spectrum (Model 501 UV Biometer Manual 2006, p. 3). This instrument is a continuation of Robertson-Berger Weatherproof meter, (Model 501 UV Biometer Manual, 2006, p. 2) and is one of the more common detectors used for routine measurements of biologically effective solar UV radiation (Huber et al. 2003).

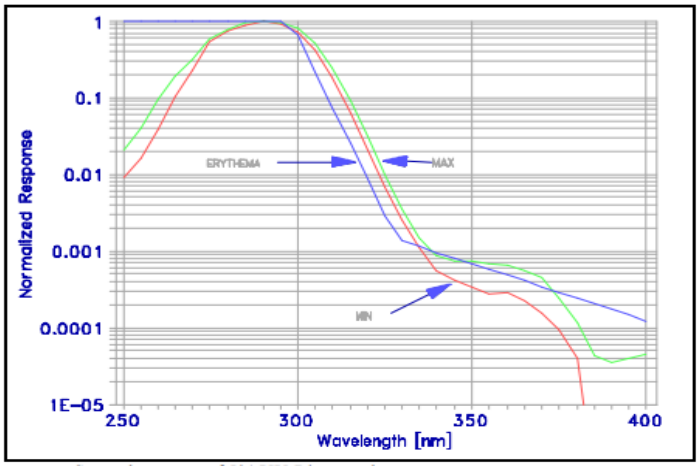

Figure 1-9: Spectral response of 501biometer detector (Model 501 UV Biometer Manual, 2006, p. 3).

Spectral sensitivity of broadband meters is influenced strongly by the detector's internal humidity (Huber et al. 2003). To maintain the stability of the instrument for a long period,

the desiccant should be replaced every 2 or 3 months (Huber et al. 2003).

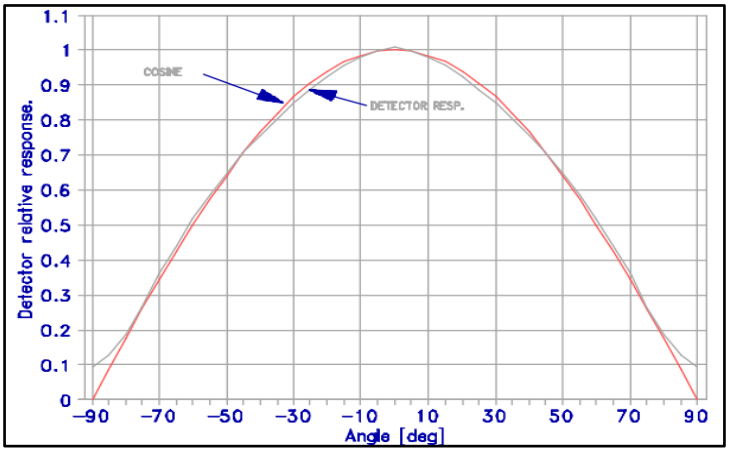

Figure 1-10: Angular response of UV Biometer detector (Model 501 UV Biometer Manual 2006, p. 4).

To measure the available global solar radiant exposure, broadband meters must follow the cosine law (Leszcynski 2002). This allows for the accurate measurement of the direct solar and also the surrounding diffuse solar radiation. Figure 1.10 shows the cosine response of the 501 UV biometer (Model 501 UV Biometer Manual 2006). UV 501 Biometers (Solar Light Co., PA, Philadelphia) that is installed at the University of Southern Queensland to monitor the erythema weighted UV, the erythemally weighted diffuse radiation and the UVA radiation over time.

1.6.1.2 Spectroradiometers

Spectroradiometers are instruments used to measure direct and diffuse UV irradiance at a high wavelength resolution (typically 1 nm) (Dahlback 2008). An example of a spectroradiometer is the MS 701 (Nozawa et al. 2007). Spectroradiometers are very sensitive instruments. They take a long time to complete a spectral scan, typically several minutes (Envall et al. 2006).

Spectroradiometers comprise entrance optics, monochromators, a detector, control and data acquisition units. Figure 1-11 shows a schematic drawing of the common components of a spectroradiometer.

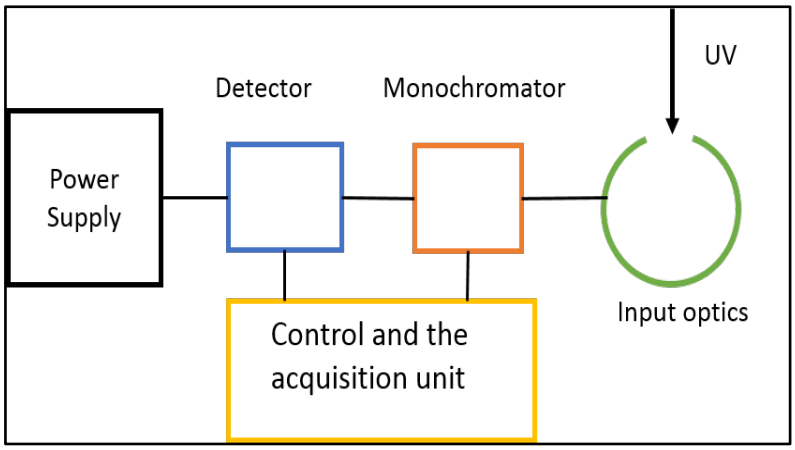

Figure 1-11: Schematic drawing of the components of a spectroradiometer.

The input optics depolarise the incident radiation before it enters the slit of the monochromator (Diffey 2002). The input optics may be either a diffuser or integrating sphere (Diffey 2002). As with broadband meters, it is important for spectroradiometers to have a good cosine response. Cosine response errors can cause errors in the global spectral irradiance measurement and a correction to the cosine response may need to be applied (Parisi et al. 2004). Diffusers are made from materials such as quartz, Teflon or PTFE (polytetrafluoroethylene), and integrating spheres are made with a highly reflective internal surface provided by a material such as barium sulphate.

The monochromator's role is to prevent measuring the radiation with the wavelengths outside the desired band (Wainwright 2012, p. 15). A diffraction grating is the part of the monochromator that disperses the incident radiation (Diffey 2002) before it enters the

detector of the spectroradiometer. The detector is a photomultiplier tube or solid-state detector. The detector's role is to sample the radiation for each discrete wavelength being measured (Wainwright 2012, p. 15). Irradiance calibration to lamps of known irradiance converts the detector signal to units of radiant exposure. Commonly used calibration lamps in solar spectroradiometry include quartz tungestun halogen (QTH) and deeuterium lamps.

1.6.1.3 Comparison between radiometers and spectroradiometers

The cost of a typical spectroradiometer ranges between $40,000 and $150,000.; however, the cost of a typical radiometer is $4000 to $6,000 (Solar Light Co n. d., p. 10). Moreover, in terms of maintenance, the radiometer does not need an operator, with the only routine maintenance being cleaning and seasonal calibration. Both types of instruments have a wide field of view depending on their input diffuser (around 160°), and difference in sensitivity (Nozawa et al. 2007).

1.6.2 Personal UV radiation measurement (UV dosimetry)

Humans are exposed daily to UV radiation by natural and artificial sources. This includes differences in exposure pattern due to both indoor and outdoor exposure time and frequency. Patterns in exposure influence susceptibility to negative health effects, including skin cancer, make personal UV radiation measurement very important to public health. Given Australia has one of the highest skin cancer rates in the world, better personal data is needed to inform the public for different situations. Thus, monitoring personal UVR exposure is an important public health initiative for populations at risk of skin and eye disease (Knuschke & Barth 1996).

Dosimeters are small instruments that are easy to carry or move. They are used to monitor

personal UV exposures. Thus, these devices are typically small in size to enable measurement of radiant exposure, often on various places of the subject at the same time (Webb 1998). Various types of dosimeters are used to monitor personal UV exposure. One of the common devices that has been used to measure UV exposure is a polysulphone (Davis et al. 1976).

1.6.2.1 Polysulphone dosimetry

Polysulphone was first developed as a UV dosimeter in 1976 by Davis et al. (Diffey 1977). Since that time, the polysulphone dosimeter has been employed for measuring environmental and artificial UV radiation (Diffey 1984). Polysulphone/polysulfone is a photo-active chemical material that has been employed for dosimetry because its spectral response approximates the erythema action spectrum (Parisi et al. 2004). The chemical structure of the polysulphone can absorb radiation in the UV band (Kollias 2010). Polysulphone's chemical structure is shown in Figure 1-12 and a picture of a manufactured

polysulphone dosimeter is shown in Figure 1-13.

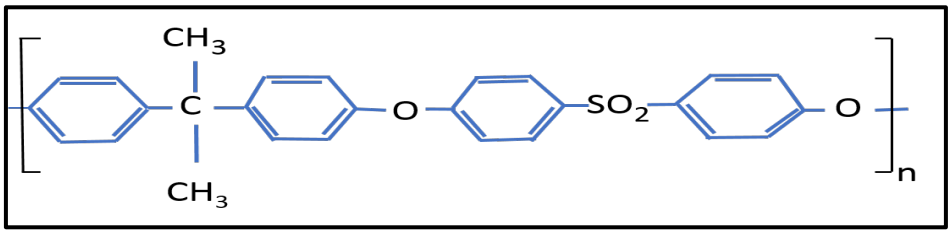

Figure 1-12: Polysulphone chemical structure (Geiss et al. 2003).

Figure 1-13: A polysulphone film dosimeter measuring 15 x 10 mm.

Polysulphone undergoes photo-degradation when exposed in a thin film form to UV radiation. The degradation occurs because of the alteration in the UV absorption spectrum of the film (Casale et al. 2009).

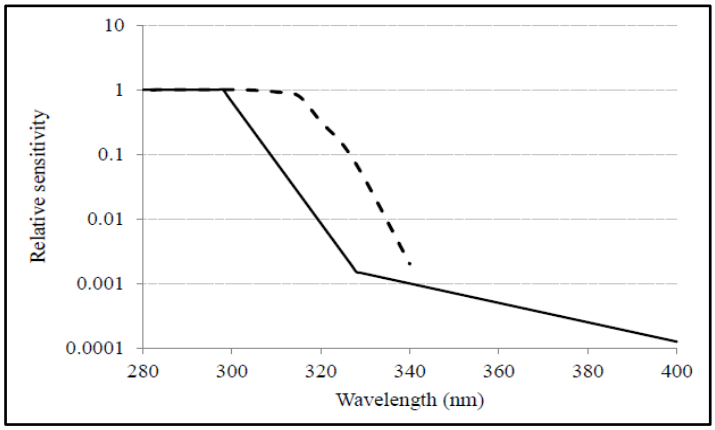

Figure 1-14: Polysulphone spectral response (dashed line (CIE 1993)) compared to the erythema action spectrum (solid line (CIE 1998)).

The polysulphone dosimeter has a spectral response that approximates the erythema action spectrum (Kollias 2010). The dashed line in Figure 1-14 shows the polysulphone response is higher in the range of wavelengths between 280 and 320 nm; after that, the response declines quickly (Parisi 2004).

1.6.2.1.1 Calibration of polysulphone dosimeters

To control the problem of some differences between the erythema action spectrum and the polysulphone spectral response, polysulphone dosimeters require calibration to the source spectrum (Parisi et al. 2004).

The calibration procedure is performed by exposing groups of polysulphone dosimeters to solar UV radiation for different periods of time while simultaneously measuring the UV irradiance with an accepted standard measuring instrument (typically a UV spectroradiometer or radiometer) at specific intervals. After that, the change of the absorbency of the polysulphone film at 330 nm is measured and plotted against the measured erythema exposure of the dosimeter film to obtain a calibration curve (Parisi et al. 2004) where the biologically effective UV erythema exposure is calculated by application of Equation 1.3, p. 15.

Figure 1-15 shows an example of a polysulphone calibration curve. It can be seen in the figure that the polysulphone starts to saturate at higher exposures, because of the protective filtering effect of the products of photodegradation. This can limit the range over which polysulphone film dosimeters can be used.

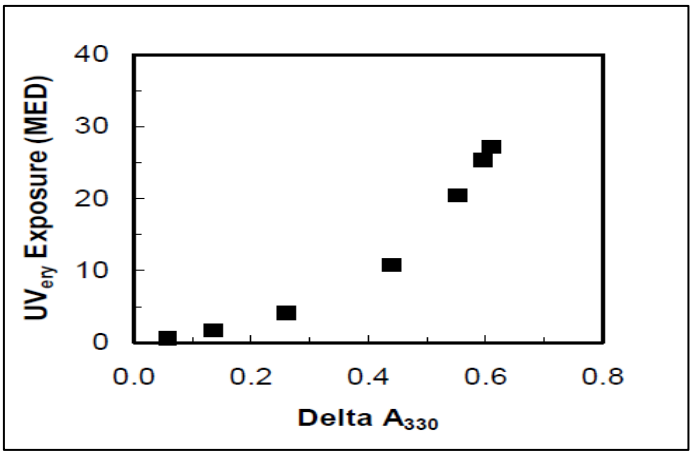

Figure 1-15: Polysulphone calibration to the UV solar irradiance in the Australian summer (Parisi 2004).

Polysulphone dosimeters can be used typically for 3 to 6 hours in summer. Used in this way, however, polysulphone dosimeters must be replaced for periods of exposure that exceed one day. This increases study costs and effort, particularly for studies with a larger number of participants (Parisi & Kimlin 2003).

There are other dosimeters, such as polyphenyline oxide (PPO) film (Schouten et al. 2010), solvent cast polyvinyl chloride (PVC) (Amar & Parisi, 2013), dual calibrated dosimeters (Wainwright et al. 2016), phenothiazine UVA dosimeters (Parisi & Kimilin 2005b) and spore film filter types of biological dosimeters (Horneck et al. 1993), such as VioSpor. Each are calibrated using a similar technique to the polysulphone dosimeter.

The PPO dosimeter has been employed to monitor UV in different environments and has the advantage that it saturates at a slower rate than polysulphone (Schouten et al. 2010). PPO can be used for up to five days in summer before requiring replacement (Amar & Parisi 2012). The PVC dosimeter is a recently developed chemical dosimeter that has an even larger dose capacity, resulting in its ability to record radiant solar UV exposures extending over 3 weeks in the summer session (Amar & Parisi 2012). Dual calibrated

dosimeters utilise a combination of PPO and polysulphone to measure erythema and vitamin D effective exposures simultaneously (Wainwright et al. 2016).

VioSpor dosimeters are a type of sensitive biological spore film filter device for monitoring the biologically effective UV radiation. VioSpor dosimeters have been used to measure the radiant exposure of construction workers in Valencia, Spain (Serrano et al. 2014). These dosimeters have various advantages that make them suited to different applications; advantages include longer exposure times, and sensitivity to different biological responses. However, the cost of manufacture and need for accurate calibration often limits their use to studies involving a small number of participants.

1.6.2.2 Electronic dosimeters

Electronic ultraviolet dosimeters employ a wide range of photodiode sensors sensitive to UV radiation (Seckmeyer et al. 2012). Electronic UV dosimeters have been employed for many studies in New Zealand (Allen & McKenzie 2010). Another common personal electronic UV dosimeter is the Sun Saver. This dosimeter contains a sensor, data logger and battery. The dosimeter is employed to measure time stamped UV exposures (Thieden et al. 2004). Typical electronic dosimeter sizes are 35 mm by 13 mm and their weight is around 20 g. Their small size allows them to be worn by study participants on wrist or arm straps. Typically, the detector is a photodiode type based on aluminium gallium nitride (AL27Ga73N) (Allen & McKenzie 2010). Electronic dosimeters may be employed to measure erythema UV exposure at high sample rates (Seckmeyer et al. 2012). Electronic UV dosimeters currently in use can record measurement at frequent time intervals and they can store data for approximately 12 days (Liley et al. 2010). Commercially available UV electronic dosimeters, such as the Scienterra range sell for approximately $450 each

(Scienterra 2019). This type of dosimeter is used commonly in research applications to measure personal exposure at the lapel, or wrist site (Allen & McKenzie 2010, Liley et al. 2010, Sherman, Z. 2014, Dobbinson et al. 2016;). If desired, these dosimeters can store data for more than 12 days, depending on the chosen sample resolution. The resolution and amount of data able to be stored in an electronic dosimeter gives them a significant advantage over traditional polymer and biological spore type dosimeters; however, collection of a large amount of data can make data interpretation difficult (Liley et al. 2010).

In terms of calibration, each electronic UV dosimeter has to be calibrated separately with the reference device, and this process takes a long time and can be expensive (Seckmeyer et al. 2012). As UV electronic dosimeters require individual calibration, using them for a large population is often impractical. Electronic UV dosimeters, employing UV sensitive photodiodes, can be reused, but they are more expensive than the traditional polymer type dosimeter, costing a few hundred dollars each. In addition to that, to determine sun exposure patterns with sun exposure, sun diaries need to be employed with electronic UV dosimeters to record sun exposure patterns and behaviours indoors and outdoors. Without sun diaries with electronic UV dosimeters, timing of sun exposure activities and behaviour would be difficult to be determined. This leads to the need for Electronic Sun Journals instead of the traditional paper-based sun diary.

Unlike UV photodiodes which form the basis of all electronic UV dosimeters, infra-red (IR) photodiodes are common due to their widespread applications in electronics. IR photodiodes are employed in this project as an Electronic Sun Journal (ESJ) and as a cost-effective replacement for UV photodiodes. Using a common IR photodiode, it is possible

to gather personal exposure information including time and personal duration outdoors. Their use also eliminates the need for paper-based sun exposure diaries, typically filled in by sun exposure study participants.

1.7 Advantages of the personal electronic sun journal (ESJ)

The traditional polymer dosimeter used by UV radiation researchers is limited by the number of participants that can be sampled. Furthermore, the use of UV photodiode electronic dosimeters is limited by the number of electronic dosimeters that can be used in any study because of their cost. The saturation limits of film dosimeters including polysulphones, restricts the length of the study period, and their use can also increase study costs.

The ESJ developed for this research project introduces a novel methodology for sensing outdoor exposure patterns not previously tested for by personal solar exposure monitoring. This technology offers a substantial cost saving over existing UV photodiodes where the ESJ also replaces the traditional paper-based sun journal while retaining the advantages of high electronic sampling rate. The developed ESJ uses an infrared photodiode that is optimised to detect periods of outdoor exposure, given the abundance of naturally occurring infrared radiation in sunlight and its relative absence in indoor locations. When connected to a suitable data logger (smartphone or portable logger), the ESJ is designed to accurately monitor personal outdoor behaviour patterns.

1.8 Research Goals

The main objectives of this research project are:

1. To develop a new personal electronic sun journal (ESJ), employing an inexpensive infrared photodiode.
2. To test the traditional infrared photodiode to determine whether it can be utilised as a personal electronic sun journal for characterising personal UV exposure

patterns.

3. Replace paper-based sun journals (self-reported volunteer recall) to complement existing exposure monitoring in UV research studies for estimating periods of exposure and personal exposure patterns.

4. To determine personal exposure patterns and the time spent in three states: (1) indoor conditions, (2) full sunlight conditions, and (3) semi-shaded environments.

Chapter 2: Materials and Methods

2.1 Diode Testing and Selection

As a first step to this project, a group of low-cost photodiodes were ordered and tested for their physical response and compatibility with a 3 V supply and data-logger unit. These photodiodes were chosen due to their cost effectiveness (ranging between 3c and $2.50 each), their sensitivity to infrared radiation (peaking at 950 nm) and their cosine response (as listed by the manufacturer). They included BPW83, BPW41N, BPV22F, SICWS4015-18 and FE.MD7100X01 infrared photodiodes from different manufacturers including Vishay (https://www.vishay.com) and TEMIC Semiconductors (www.elnec.com). The photodiodes were tested in a voltage difference circuit consisting of a 3 V battery and a 56 kΩ resistor (Figure 2-1). A photography lamp and oscilloscope were also used to measure the voltage output difference under different light conditions. A large resistor was chosen to save the battery life by minimising the circuit current when in operation.

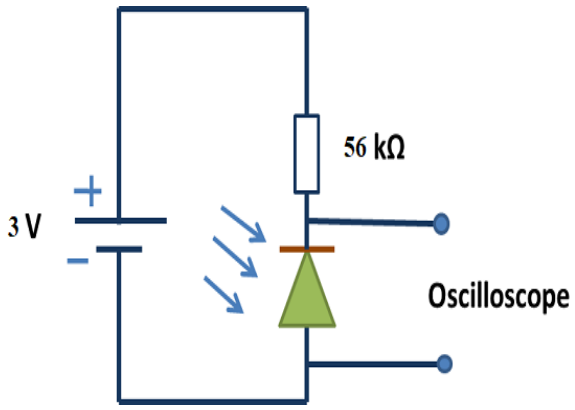

Figure 2-1: Diagram of the photodiode circuit.

Each photodiode was tested in terms of maximum and minimum output voltage, temperature stability and cosine response. Maximum and minimum voltages were tuned by the selection of the resistor such that output ranged from 0 to 2.5 V. This voltage represents the maximum range of voltage able to be recorded by a monitoring data logger (Tinytalk TK-4703 voltage data logger, Gemini Data Loggers, UK), which was selected to obtain the highest possible voltage resolution of the circuit output when operated as a standalone electronic dosimeter. The maximum and minimum voltage values were tested by placing the photodiode circuit in front of a halogen photography lamp, where turning the lamp on gives the minimum voltage monitored at A (Figure 2-2a) due to diode saturation and turning the lamp off gives the maximum circuit voltage due to the diode restricting current flow in the circuit (Figure 2-2b).

The photodiode offers very low resistance when light is incident upon it because current flows from the cathode (A) to the anode (B), so the output voltage drops to zero. The opposite occurs when there is no light incident on the photodiode. In this condition, the photodiode offers a resistance that is much higher than that of the resistor, with a small current flowing between the anode (B) and the cathode (A). Thus, the output voltage is higher under conditions of no light and low when light reaches the diode surface.

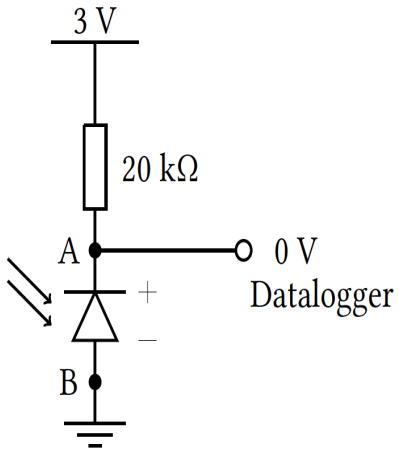

(a) *Saturated infrared exposure state.*

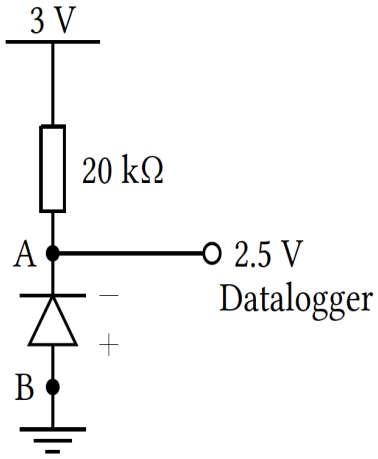

(b) *Limited infrared exposure state.*

Figure 2-2: Circuit design and operation under saturated and limited exposure states. Maximum output current occurs when the diode saturates and is limited to less than 0.1 mA for long battery life.

The operation of the photodiode detector is based on the principle of the photoelectric effect, where the generated electrons and holes remain inside the absorbed semiconductor material. The photoelectric effect occurs when a photon is incident upon a bonded electron with an atom in the absorbing semiconductor material. The electron absorbs the total incident photon energy and is emitted from the surface of the material. The emitted electron is called a photoelectron (Figure 2-3). This effect occurs when the energy of the incident photon is greater than the released electron binding energy.

The semiconductor photodiodes tested in this project are a P-N junction structure. The P-N junction is prepared by connecting a P type semiconductor with an N type semiconductor. Figure

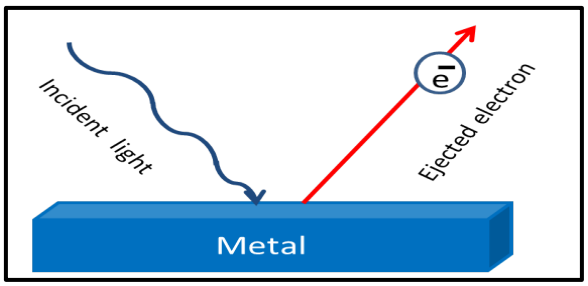

Figure 2-3: Diagram of the photoelectric effect.

2.4(a) below shows the P-N junction to form a diode. At the boundary of the junction, the region depleted of charge because of the drift of opposite charge carriers forms on both sides of the boundary and cancel each other. This drift of charge across the boundary causes an imbalance in the total charge of the semiconductor lattice, leaving positive charge in the side of N type material at the boundary and negative charge at the side of P type material. Thus, this leads to the induction of the electric field (E) with the direction from N type to P type across the boundary as shown in Figure 2-4(b). The induced electric field prevents any further drift of charge across the boundary.

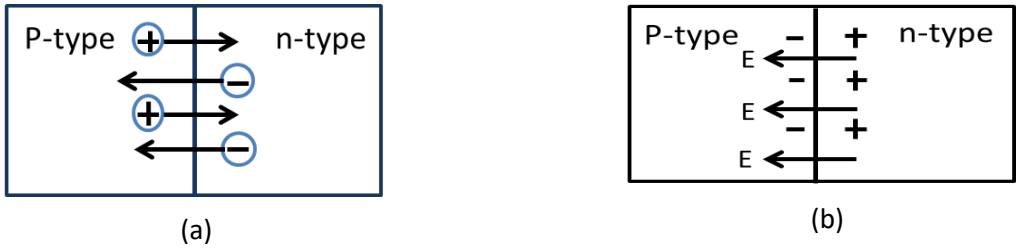

Figure 2-4: Diagram of P-N Junction.

The P-N junction can be connected to a battery in two ways: forward bias and reverse bias. In the forward bias method, as shown in Figure 2-5(a) and Figure 2-2(a), the N type material is connected to the negative part of the battery and the P type material is connected to the positive part of the

battery. In this situation, the positive part of the battery drives out the positive charge carriers in the P type material and the negative part of the battery drives out the negative charge carriers in the N type material, thus the electrons and the holes combine in the junction. At the same time, the positive part of the battery pulls electrons off the P type material, generating holes, and the negative part of the battery gives supply to the electrons in the N type material. So, current passes continuously because of the charge flow. In the reverse bias method, the polarity of the battery is reversed, meaning that the negative part of the battery connects to the P type material of the junction and the positive part of the battery connects to the N type material of the junction as shown in Figure 2-5(b) and Figure 2-2(b). In this case the battery makes the electrons in the N type material and holes in the P type material move away from the junction. This leads to increasing potential across the junction until it opposes the battery potential. The current through the diode in this condition is very small.

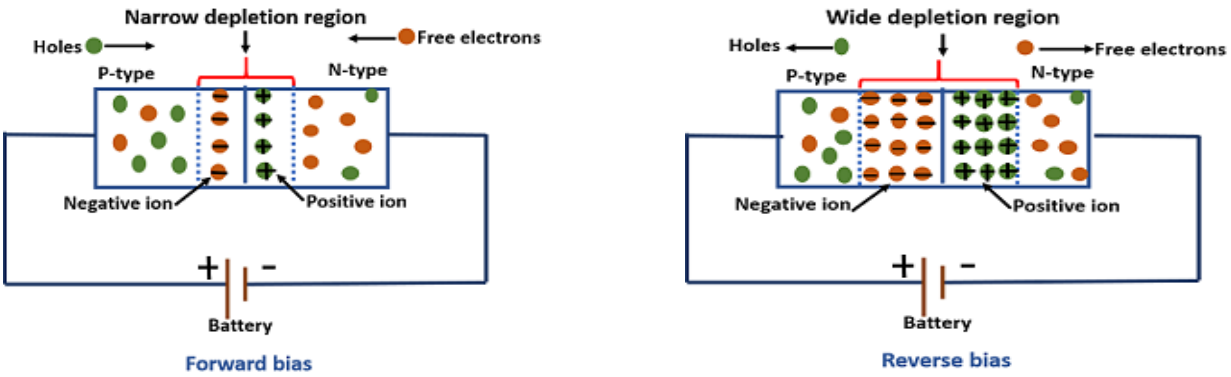

(a) (b)

Figure 2-5: (a) The diode has a forward bias (b) The diode has a reverse bias.

Presenting the previous explanation about the photodiode detectors has demonstrated the science of the photodiode as the light strikes the photodiode surface. This is based on the photoelectric effect. The previous explanation also showed how the photodiode works in forward bias and reverse bias, as the BPV22F will be connected in reverse bias in the designed ESJ circuit.

2.1.1 BPV22F Photodiode

After testing the photodiodes, the photodiode with the best cosine response was chosen. The cosine response of the dosimeter reflects the alteration of its response with the changing angle of the incident radiation. A well-designed dosimeter will provide a maximum signal when the maximum irradiance occurs at a radiation incident angle where θ equal to 0°. As the angle of incidence increases, the irradiance decreases by the factor cos θ (Parisi et al. 2004). The cosine response of the dosimeter should, therefore, follow the curve of the cosine function. The variation between them is the degree of error. To minimise the potential error due to cosine response, a BPV22F (Vishay) photodiode was selected for use in the ESJ circuit. This photodiode is available from electronics suppliers at a cost of 58c each. The BPV22F is designed by the manufacturer for high

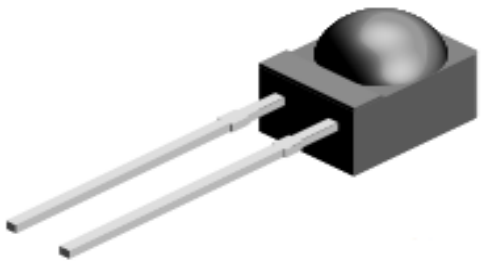

radiant sensitivity over wide receiving angles, is small and lightweight (measuring 4.5 x 5 x 6 mm)

Figure 2-6: The shape of BPV22F photodiode (BPV22F data sheet, Vishay semiconductors company 2017).

and has a radiant sensitive area of 7.5 mm^2. Figure 2-6 below shows the shape of BPV22F photodiode.

The photodiode is sensitive to the Infrared A waveband (from 870 to 1050 nm, peak response 950 nm). When operated in a reverse bias state and exposed to sunlight, the diode response saturates as illustrated in Figure 2-2(a).

Conversely, in densely shaded environments or under indoor fluorescent lighting, which experience a naturally limited infrared irradiance, the diode response is minimised. The photodiode when worn as a personal ESJ can, therefore, record periods of indoor and outdoor exposure time, where the diode output voltage is monitored by a data logger and the erythemally effective UV exposure measured simultaneously by a calibrated broadband UV meter installed in proximity to the wearer.

2.2 Circuit Design and Sensitivity Testing for Different Light Intensity

The ESJ circuit was designed for cost effectiveness and design flexibility. All the circuit components are interchangeable. The initial circuit setup included a 56 kΩ resistor. However, the change in the output voltage was tuned using different resistors to note differences in light intensity so that the minimum output voltage of 0 V was found only under the highest light level, where light intensity was varied by placing a halogen photography lamp (which emits radiation from visible radiation to infrared radiation) at different distances from the photodiode. This allowed detection of light levels at voltages above 0 V up to minimum light levels of just below 2.5 V. In this way, different light intensities could be monitored under controlled laboratory conditions. Near midday, under cloud free conditions the natural solar IR-A (760-1400 nm) spectrum peaks

at 300 W m^{-2} (Barolet et al. 2016). Therefore, tests performed in the laboratory under the halogen photography lamp should show that the ESJ will work under the greater intensity of solar IR radiation. After laboratory testing, the ESJ was placed in various outdoor environments (see section 2.3). The resistor chosen in the final circuit design was a 20 kΩ resistor. This resistor, along with the 3 V battery and a Tinytalk TK-4703 voltage data logger (Gemini Data Loggers, UK) used to monitor the voltage level are the final elements of the circuit developed in this project. Figure 2-7 shows the diagram of the circuit developed for use as an electronic sun journal (ESJ).

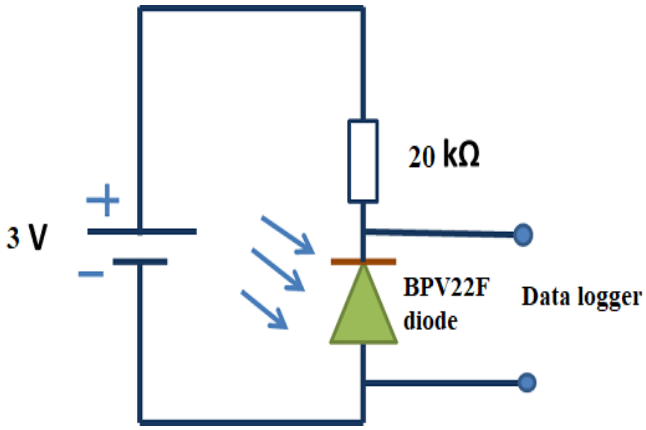

Figure 2-7: The designed photodiode circuit.

The data logger used in this project monitored voltage as pulses between 0 to 2.5 V every second. The TK-4703 has a memory capacity of 16 kilobytes and in this configuration could log continuous sunlight levels for 4.5 hours. As designed, the total monitoring period is dependent on the flexible sampling rate of the ESJ and the available memory of the data logger unit. The ESJ output can be monitored at very high temporal resolutions or it can be lowered for studies that require monitoring over longer periods.

To initialise the logger unit and read the voltage, the logger was connected to a computer with a USB cable. Tinytag Explorer software (Version 4.9) was used to present the recorded voltage data.

This data was copied and stored in CSV (comma-separated values) format for later data analysis. Although a Tinytag data logger was used in this project, other forms of portable logger units have the potential to be used with the designed photodiode circuit. These may include smartphone memory or micro-SD cards, or miniaturised computers, or other commercially available data loggers. These alternative data logger units are more affordable than many commercial voltage data loggers but may require further assembly depending on the logger design. Alternative purpose-built data loggers require at a minimum an analog to digital converter to convert a small 0–2.5 V signal to an eight-bit digital value that can be stored on an SD card, EPROM, or alternative portable memory system such as a USB memory stick. Small microcontroller units designed to sample the ESJ voltage at user specified intervals are therefore capable of greatly extending the storage range of the device, depending on the number of bytes of data storage available. Many DIY data logging kits and designs are made freely available on electronics forums accessible from the internet and would make very reasonable substitutes for commercial data loggers. Excluding the data logger, the complete ESJ circuit can fit within the circumference of a 3 V coin cell battery (measuring 20 mm in diameter). The design of a small transducer circuit could be optionally included to send monitored voltage signals digitally to off-site storage systems through the use of WI-FI to nearby computer or personal data storage devices, including smartphone or portable tablet systems.

2.3 Preliminary Environment Tests

A circuit prototype was developed on a project board for testing as shown in Figure 2-8 below.

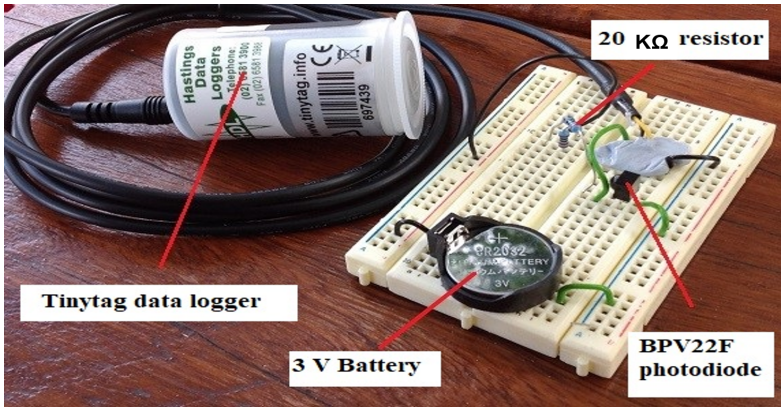

Figure 2-8: Picture of the prepared circuit in the laboratory.

This circuit was then tested in saturated exposure conditions (full sun) and limited exposure conditions (indoors).

When the circuit voltage was monitored inside the lab (dark condition), the data logger recorded the maximum voltage as there is limited available infrared radiation indoors. Under this condition, the photodiode acts as a resistor and the voltage will reach the maximum value (2.5 V). The connected circuit was tested indoors for 15 minutes before testing outside to ensure the correct operation. A monitored response of 2.5 V over 15 minutes when it was left in the dark state confirmed that the circuit was operating correctly. Similarly, when it was placed in the open sun for a period of 15 minutes, the 0 V level was also confirmed**.** This range of the output voltage (from 0 V to 2.5 V) is appropriate for the purpose which the circuit is designed for. Because the purpose is measuring the exposure patterns and to determine if the ESJ user is in full shade, full sun, under tree shade or under a shade structure.

2.4 Cosine Response

The cosine response and signal output of the photodiode circuit was tested to determine the ability of the ESJ measurement to reflect ambient exposure conditions, including differently shaded environments likely to be experienced during field trials. Manufacturer's data sheets for the BPV22F show the diode response matches the natural cosine function from 0 to 80° (Figure 2-9).

The cosine response of the BPV22F photodiode was tested against a shielded infrared light source. The test source was a 100 W infrared lamp shielded by a large 40 x 40 cm plate with a central aperture of 7 mm diameter that allowed incoherent radiation to reach the photosensitive surface of the diode. The photodiode circuit output voltage at A (Figure 2-2) was monitored by oscilloscope during this test as the diode was rotated in steps of 10° through angles of incidence ranging from 0 to 80° using a fixed rotating stand and clamp assembly positioned 5 cm from the shield and the source aperture.

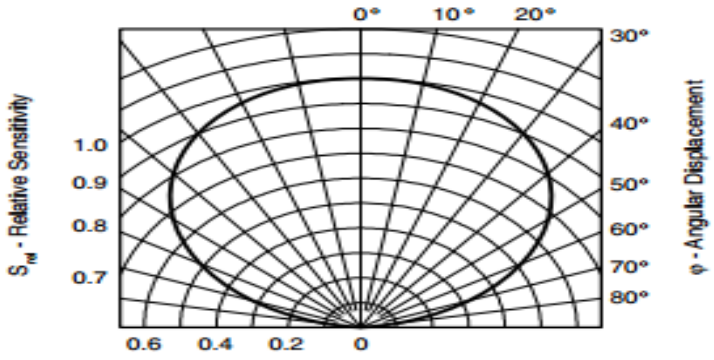

Figure 2-9: Cosine response of the BPV22F photodiode (manufacturer's data).

2.5 Temperature Stability Test

A temperature stability test was also performed to check the photodiode response for given changes in ambient temperature likely to be experienced by the users of the ESJ. The test was performed by placing the circuit under a filtered infrared lamp. Under these conditions, the output signal voltage was maintained between the maximum and minimum voltage levels by filtering the radiation source to ensure the output signal could be monitored between the ESJ voltage range of 0 to 2.5 V. Once a stable voltage was found after filtering the source, the ambient temperature of the diode was adjusted by steady heating with a hair dryer to detect variations in output voltage.

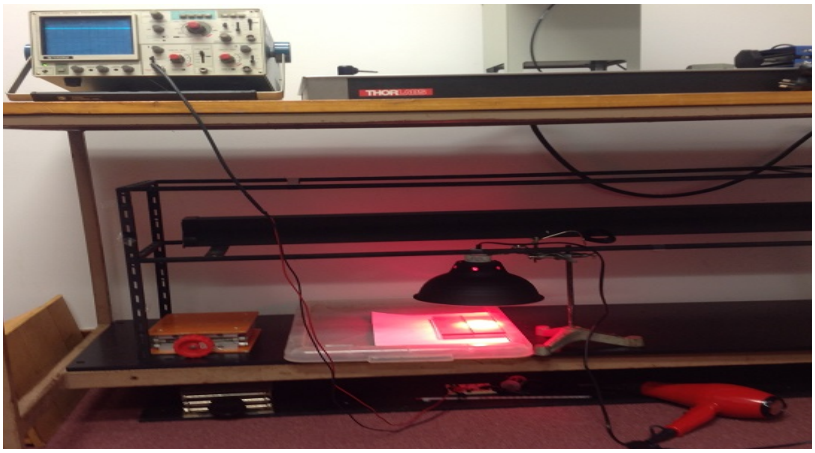

Figure 2-10: Temperature stability test setup.

An oscilloscope was employed to read the photodiode voltage output. Figure 2-10 shows the circuit set-up. To allow the ambient air to cool by leaving the air conditioner on overnight, the experiment set-up was prepared the day before, the air conditioner was adjusted to 16°C. In addition to that, the next morning an ice container was placed next to the circuit before heating with the hair dryer unit. The ambient temperature of the photodiode was measured with a mercury thermometer.

During the test, the infrared lamp was turned on and the voltage reading was recorded from the oscilloscope to produce a plot of temperature vs voltage from 16°C up to 60°C.

Figure 2-11: Skyview test experimental setup.

2.6 Skyview Test

The BV22F response saturates in natural sunlight where direct solar radiation reaches the photosensitive area of the diode. To determine the influence of diffuse solar radiation on the diode, an open-air sky view test was performed by measuring the photodiode output voltage while it was shaded by a shade square 113 mm x 113 mm which was progressively lifted every 1 minute from in height increments of 7.5 mm 0 to 150 mm above the circuit photodiode. A picture of the experiment is shown in Figure 2-11.

The test was performed under cloud-free midday conditions. Here the sky view was approximated according the equation:

$$S\% = \frac{100}{2\pi}\,[2\pi - 2\pi(1 - sin\theta)] \qquad (2.1)$$

where the percentage sky view, $S\%$, assumes a hemispherical field for diffuse skylight of nominal radius 1 which is shaded by a square shadow of side length $2r_\theta$ as shown in Figure 2-12(b) below. The variable r_θ is a function of the shade shield height (h) and is calculated according to Equation 2.2.

$$r_\theta = \cos\left(90 - \ tan^{-1}\left(\frac{56.5}{h}\right)\right) \qquad (2.2)$$

Where h, the height of the shield, is also shown in Figure 2-12(a). In the approximation of $S\%$, the sky view was covered by the shield shadow to prevent radiation from the upper hemisphere (as indicated in the red area of Figure 2-12) from reaching the diode. In all calculations of sky view, the size of the shadow is dependent upon the height of the shield, h (in mm) above the photosensitive surface of the infrared diode where the radius of the hemispherical sky view will always be 1 irrespective of shield height. Here the maximum length of r_θ will be 1 when the shield is 0 mm above the diode surface and will reduce in proportion to the visible sky view as h increases.

The factor [2π-2π(1-sinθ)] is the proportion of sky hemisphere available to the photodiode when shaded by shield in Figure 2-12. That is, 2π(a sky hemisphere of nominal radius 1, assuming correctly that the hemisphere area is 2π1^2) subtract the hemispherical sky area defined by a spherical cap (red area in Figure 2-12(b)). The area of a spherical cap is defined as 2πr c where c is the remaining length of the spherical radius, r after subtracting h. This length is shown in Figure 2-12(a), and that c will be (1-h) from Figure 12-2(a) or as stated in the formula (Equation 2.1) above (1-sinθ) because the hemispherical sky is set at 1, and the height of shield, h can be defined as (h/1), where h/1 is sinθ.

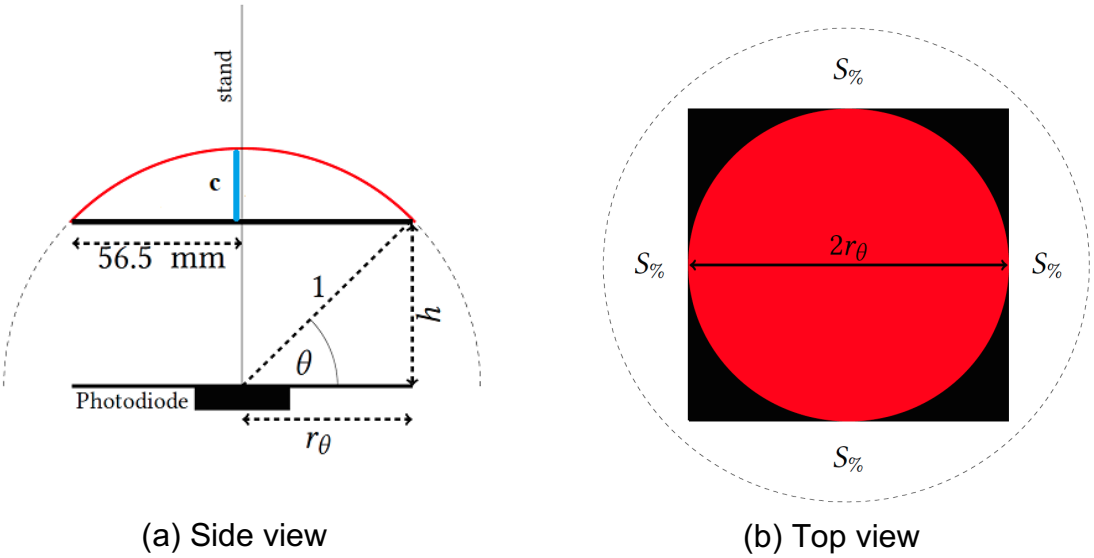

(a) Side view (b) Top view

Figure 2-12: Sky view assembly used to test the infrared photodiode sensitivity to increasing levels of diffuse solar radiation (red-shaded sky hemisphere, black shade shield, dotted – visible sky view of nominal radius 1).

For the sky-view test, the resulting voltage should vary from the maximum value of 2.5 V when the shade shield is very close to the photodiode to the minimum value 0 V when almost all of the diffuse solar radiation reaches the photodiode. The tested height range for the shadow shield was equal to an approximate range in a diffuse sky view of 0 to 99.6% measured over 21 steps (starting from 0 mm to 150 mm, with increments of 7.5 mm) (approximately 5% increments in sky view). During each step, the shadow cast by the shield attached to the stand assembly was moved such that the diode remained near the centre as indicated in Figure 2-12.

2.7 Environment Characterisation (Static Response Test)

The purpose of environment characterisation tests was to determine if the photodiode responded in different kinds of shaded environments and to determine if a difference could be found between a static shade structure, and tree canopies that provide both heavy and light shade protection. These different types of environment are the places typically occupied by people as might occur over a

day to day exposure in interval and included: an indoor environment (Figure 2-13(a)), an open environment (Figure 2-13(b)), light tree shade (Figure 2-13(c)), heavy tree shade (Figure 2-13(d)), a fixed shade structure (Figure 2-13 (e)) and a north facing verandah (Figure 2-13(f)). Each type of environment was tested separately.

2.7.1 Indoor environment

This test was conducted inside an office building at the University of Southern Queensland. Diode output was tested by placing the circuit in a stationary position and left for 15 minutes with all indoor lighting switched on.

2.7.2 Open environment

The circuit was placed in an open outdoor environment in full sun for a period of 15 minutes near midday (Spring 2016).

2.7.3 Light tree shade

Light tree shade located in the University of Southern Queensland grounds was chosen for the third static environment test. The output signal of the diode was monitored for a period of 15 minutes under light tree shade, defined as shade through which sunlight could pass and intermittently shade the ESJ.

2.7.4 Heavy tree shade

When the circuit was placed under heavy tree shade, the circuit output was monitored for a period of 15 minutes in a location where little or no sunlight reached the ESJ due to direct blocking by the overhead tree canopy.

2.7.5 Fixed shade structure

The fixed shade structure was located within the Japanese Garden, very close to the University of Southern Queensland. In this environment, the ESJ was placed on a table within the structure (approximately 0.9 m above the ground) and left for a period of 15 minutes. During this period the ESJ was directly shaded from direct solar radiation. A changing shade pattern was experienced due to movement of the solar disc during this test. This was expected to change the resulting output voltage.

2.7.6 North facing verandah

The ESJ was placed on the floor of a north facing verandah of block O1 at the University of Southern Queensland for a period of 15 minutes (Figure 2-13f). This verandah receives direct sunlight during the morning and lunch times, but is shaded later in the day. There were some trees in front of the verandah and people crossed in the front of the ESJ circuit during measurement. This was expected to affect the resulting output voltage.

(a)

(b)

(c)

(d)

(e)

(f)

Figure 2-13: Pictures of different types of environments which are typically occupied by people comprising: (a) an indoor environment, (b) an open environment (full sun), (c) light tree shade, (d) heavy tree shade, (e) a fixed shade structure and (f) a north facing Verandah.

2.8 Estimating the Eythemally Effective UV exposure

The photodiode circuit was designed as an ESJ for the measurement of personal sun exposure patterns. Tests were also conducted, however, to determine if personal erythemally effective exposure could be monitored by measuring exposure patterns with the ESJ while simultaneously measuring the ambient erythema UV exposure using a site mounted broadband radiometer. By

determining the specific time intervals outdoors monitored from personal ESJ output and then comparing these periods to the daily erythemally effective UV exposure monitored by ambient radiometers, approximate estimates of personal solar UV exposure were able to be derived.

2.8.1 Measuring ambient UV exposure

A broadband radiometer (model 501 UVB Biometer, Solar Light Company, PA, USA) calibrated to the erythemally effective UV (McKinlay & Diffey 1987) installed in an open rooftop location (Figure 2-15) at the University of Southern Queensland campus (27.5° 152°E, 693 m asl) was used to measure the ambient global (unshaded) erythemal UV exposure.

Figure 2-14: Erythemally effective five-minute exposures were monitored at the University of Southern Queensland using a broadband 501 UVB biometer (Solar Light Company PA, USA) calibrated to the erythemal action spectrum for human skin.

2.8.2 Validation field trial and individual walking tests

Personal UV exposure estimates, approximated by comparing ESJ exposure patterns to the rooftop mounted radiometer, were validated against the output of a handheld PMA2100. The PMA2100 served as a personal radiometer to measure actual UV exposure while field tests were being

conducted. This smaller, portable instrument employed a PMA2102 SUV erythemal UV detector (Solar light Company PA, USA). The calibration of this personal radiometer was performed by application of the McKinlay and Diffey (1987) erythemal action spectrum using a spectral irradiance lamp traceable to the NIST (USA) standard (manufacturer calibration date 14 August 2015). To ensure comparability of the ambient UV exposure estimates monitored against the ESJ, the fixed rooftop mounted ambient biometer was calibrated to the personal PMA2100 response. Results were expressed as erythemally effective exposures (J/m^2).

ESJ exposure estimates were designed to also test the response of the ESJ for an individual walking between and through different outdoor environments to enable classification of periods of indoor exposure, periods within shaded environments and periods located in direct sunlight.

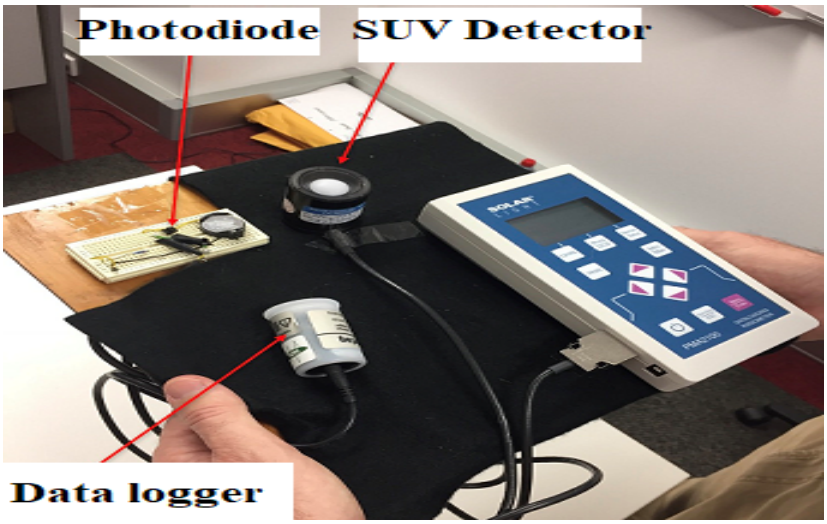

Figure 2-15: The ESJ consisting of a BPV22F photodiode (Vishay semiconductors) and data logger (Tk-4703 Gemini Data loggers, UK). During field trials, the ESJ exposure estimates were also compared against a PMA2100 radiometer with attached PMA2012 SUV detector (Solar Light Co .PA, USA).

Trials were conducted by placing the BPV22F photodiode circuit onto a wooden board (30 x 30 cm) covered with black felt to eliminate stray reflections. This held the photodiode, prototype circuit board, the data logger and PMA2102 SUV erythemal detector (Figure 2-14). A total of 5 exposure trials were conducted. Each field test varied in periods of exposure of between 1.5 and 2 hours and involved walking around 4 different stations with different shade levels. Field exposures were held at various times of day from September to March 2017 (between 7:00 am and 5:00 pm local time) and under different ambient conditions. All outdoor exposure tests were conducted at the University of Southern Queensland (Toowoomba campus).

2.8.3 Estimating exposure from biometer measurement and ESJ output

Estimates of personal UV exposure were determined by integrating the global biometer UV irradiance monitored during ESJ field tests. Exposure estimates (E_{est}(J/m^2)) were determined as the sum of global erythema irradiance monitored during each second the ESJ was operating in proximity to the field instruments. Personal exposure estimates were determined for ESJ signal voltages measured between 0 and 2.5 V according to Equation 2.3:

$$E_{est} = \sum \frac{2.5 - p}{2.5} I_{global}(t) \qquad (2.3)$$

where I_{global}[J/s/m^2] represents the UVB 501 biometer global erythema irradiance and p represents the ESJ voltage, such that during periods indoors (2.5 V), no global solar UV is included in the personal UV exposure estimate. From the equation, during periods of full sun (0 V) the full global solar UV irradiance is included in the estimate of personal exposure.

In the next chapter, the results of the presented tests will be shown. First, the outcomes of the cosine response test will be presented, followed by sky view and temperature stability test results. Preliminary environment tests measured for 15 minutes in each of six different shade environments will be presented followed by the environment characterisation tests to approximate personal estimates of UV exposure.

Chapter 3: Results

In this chapter, the outcomes of the experiments performed on the Electronic Sun Journal ESJ will be shown. These experiments include the cosine response test, sky view test, temperature stability test, environment tests and field trials for estimating personal UV exposure.

3.1 Cosine Response

The measured cosine response is compared to the nominal cosine ratio in each 10° step range from 0 to 80° inclusive (Table 3-1). The measured response up 40° deviates by no more than 13% of the normal cosine ratio. The ESJ response, as measured using the infrared lamp and aperture assembly, underestimates the nominal cosine response for angles greater than 40° and overestimates for the angles less than 40°. It is likely that there was an error associated with the measurement of the angle of incidence of the incoming irradiance with respect to the photodiode sensitive surface. The incidence of infrared irradiance on the photodiode's sensitive surface did not have accurate angles. As changing the angle of the incident irradiance by 10° was hard to perform because the ESJ was fixed on the rotating stand so as to change the angle by 10° every time, the whole ESJ circuit needed to be rotated. This resulted in the photodiode's sensitive surface not being on exactly the required angle.

*Table 3-1: Measured cosine response of the BPV22F photodiode assembled into the ESJ for increasing incidence angles, **θ**. Response is expressed as the normalised ratio of maximum saturation voltage measured between 0 and 2.5 V.*

θ	Diode response	Cosine ratio
0°	1	1
10°	1	0.98
20°	1	0.94
30°	0.98	0.87
40°	0.71	0.77
50°	0.48	0.64
60°	0.24	0.5
70°	0.06	0.34
80°	0.03	0.17

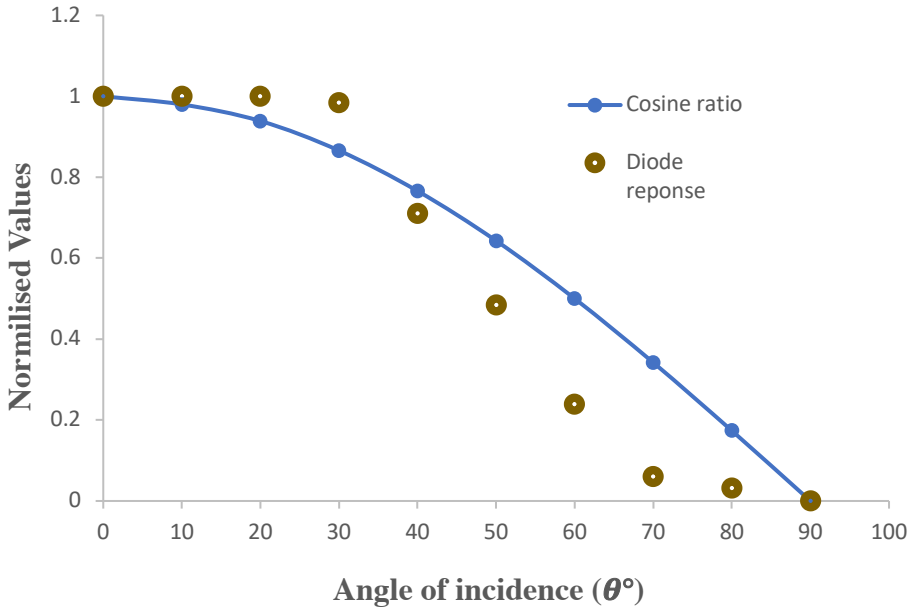

Figure 3-1: Cosine response of the BPV22F photodiode.

The cosine response of the BPV22F diode is shown by dots in Figure 3-1 above. The diode response is expressed as the ratio of the maximum saturation voltage. The blue line is the cosine ratio.

3.2 Sky View Test

The ESJ output varies with shade density. Light shade will result in low voltage (greater sky view) and dense shade will result in higher voltage (lower sky view). Figure 3-2 gives the average output voltage of the diode relative to the diffuse sky view measured using the shade shield assembly described in section 2.6. As the diffuse sky view approaches 100%, the output voltage falls to 0 V. As seen in the plot of voltage versus sky view, an open sky view sensitive to diffuse radiation will result in a small potential being recorded by the ESJ. Any further exposure to direct solar radiation will saturate the diode, resulting in a measurement of 0 V. Therefore, any monitored dosimeter readings greater than 0 V are due to either exposure to diffuse radiation in an open environment or to a combination of direct and diffuse (global) solar

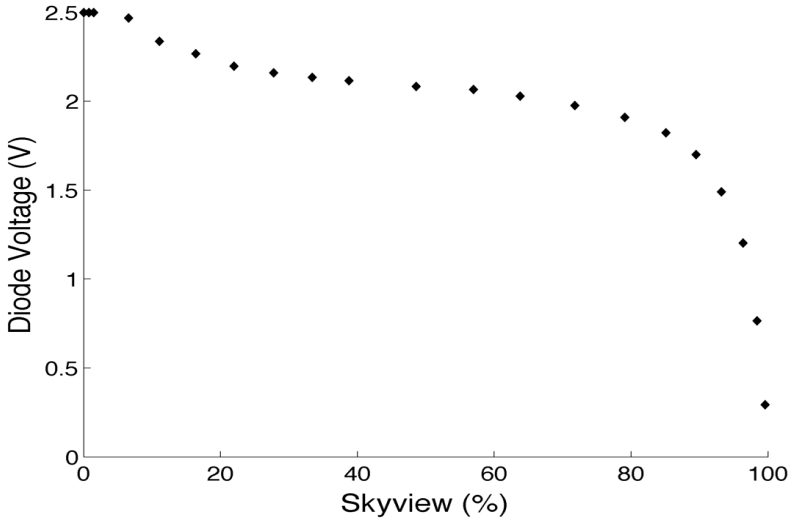

Figure 3-2: Photodiode voltage plotted as a function of sky view.

radiation. Either of these cases is accounted for by the summation of E_{min} (Equation 2.3 (Chapter 2)) and E_{max} (Equation 2.4 (Chapter2)).

3.3 Temperature Stability Test

The output voltage of the ESJ with the variation in the ambient temperature from 16 °C to 60 °C is shown in Figure 3-3.

The temperature coefficient expressed as the difference in voltage per degree Celsius from 40 to 45 °C is -0.01 V/°C. This is lower the manufacturer's temperature coefficient of -2.6 mV/°C. It is possible this occurred because of the limited range of the temperature which the BPV22F diode was tested against in the lab (16 to 60°C) as the ambient temperature could not be increased or decreased more than across this range in the lab. The results obtained show that the ESJ can be employed in normal summer and winter ambient temperatures. In addition to that, the manufacturer guarantees the BPV22F will work in temperatures ranging from -40°C to 100°C. This range is outside the expected ambient air temperature likely to be experienced in the field.

3.4 Environment Characterisation Tests

The ESJ is sensitive to the environment. The ESJ output voltage for and photographs of several static environments on the Toowoomba USQ campus are shown in Figures 3-4, 3-5, 3-6, 3-7, 3-8 and 3-9. Here the ESJ output is shown when rested on a horizontal plane and left in a stationary position for a period of 15 minutes in each environment. Characteristic of each

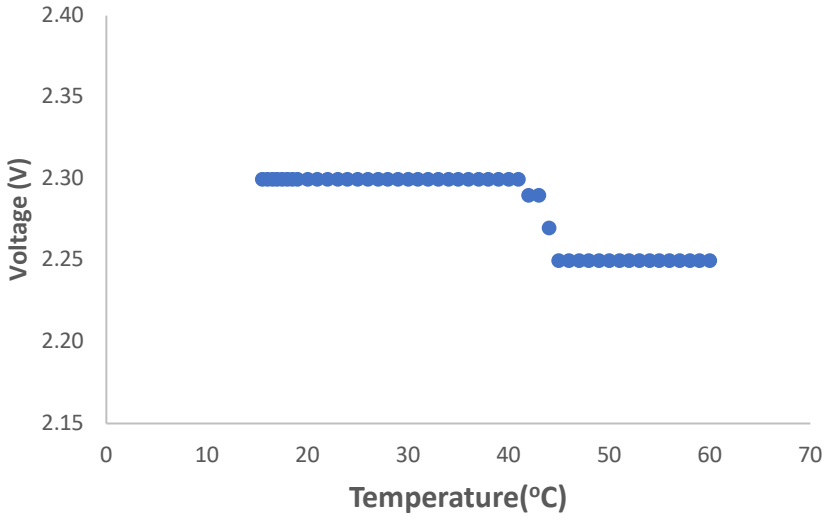

Figure 3-3: BPV22F photodiode response (output voltage) vs variation in the ambient temperature.

environment is the increased output voltage of the BPV22F with increasing shade density (reduced sky view).

3.4.1 Indoor environment

Figure 3-4(a) below shows a picture of the photodiode circuit in the first static environment, a full shade environment (inside an office in the University of Southern Queensland). The resulting output voltage is shown in Figure 3-4(b). As expected, this is a straight line at 2.5 V.

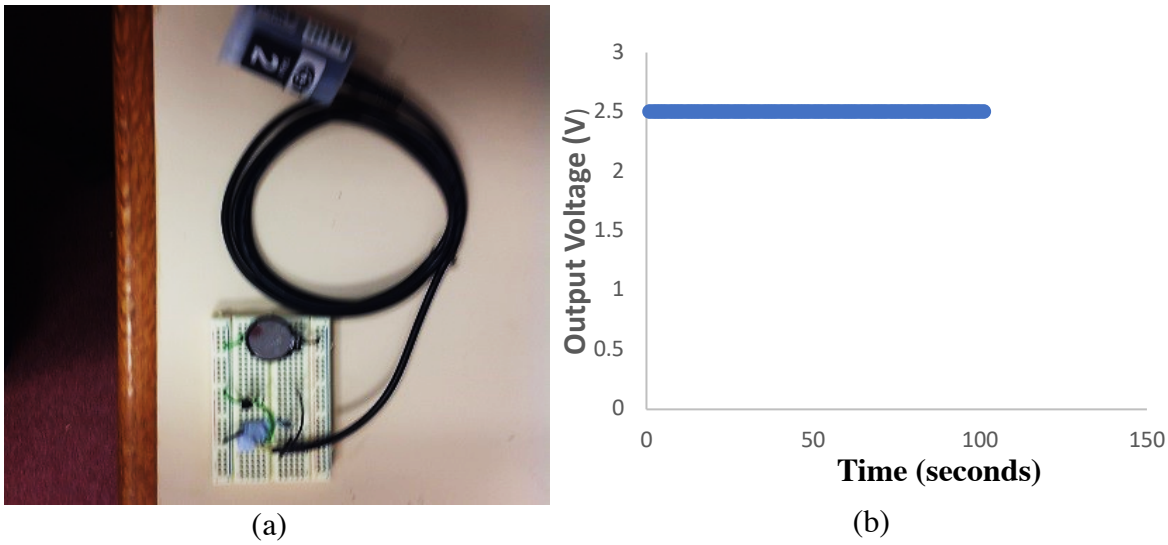

(a) (b)

Figure 3-4: (a) Picture of ESJ in the full shade environment; (b) The output voltage of the ESJ in a full shade environment.

3.4.2 Open environment

The second static environment tested is full sun. Figure 3-5(a) shows a picture of the full sun location where the test was performed, and the red circle shows where the ESJ was exactly placed during the test. Figure 3-5(b) shows the output voltage of the ESJ. The resulting voltage is a straight line at 0 V. As expected, the diode output voltage goes to zero in a condition of full sun in an open environment.

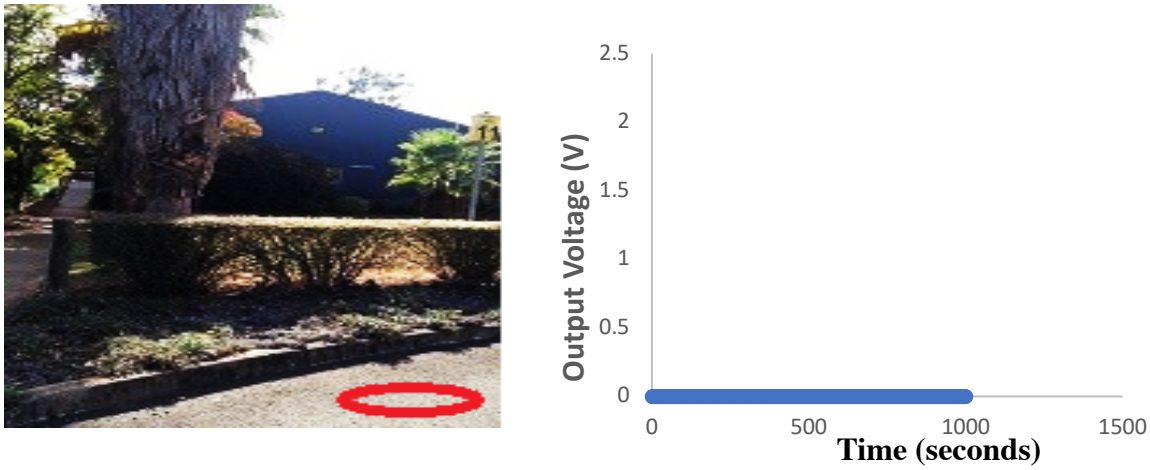

(a) (b)

Figure 3-5: (a) Picture of the second test (full sun) location, (b) The output voltage of the ESJ in a full sun environment.

3.4.3 Light tree shade

The third static environment test was performed on ground under light tree shade at the University of Southern Queensland. The tree is shown in Figure 3-6(a) and the output voltage of the ESJ is shown in Figure 3-6(b). As seen in Figure 3-6(b), the output voltage varies from around 0.8 to 1.23 V. The result shows a decrease in the output voltage as shade moves across the photodiode intermittently. The shade increases as the sky view decreases throughout the remainder of the test. Also, the output voltage in this type of condition reflects the type of test environment. The result is not a straight line as observed in the full shade condition. The signal has noticeable fluctuations, which means the environment is natural. In the signal obtained, there are some voltage values that dropped to zero. This occurred because of the movement of the tree's leaves as the weather was slightly windy on this test day.

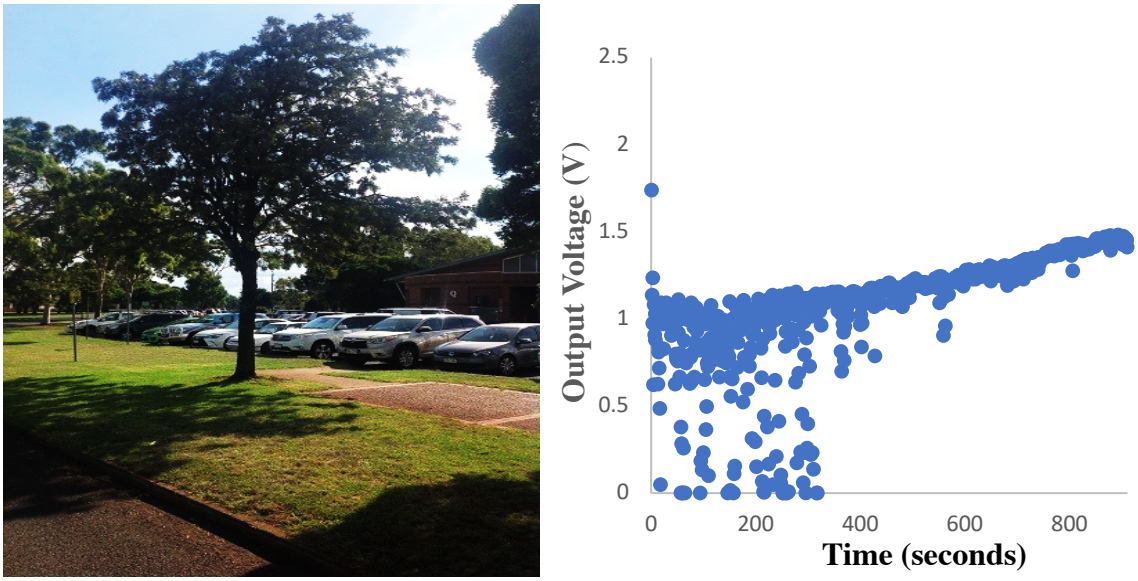

(a) (b)

Figure 3-6: Light tree shade in the University of Southern Queensland (third static environment test location, (b) ESJ output voltage in light tree shade.

3.4.4 Heavy tree shade

Heavy tree shade was chosen as the forth type of static environment. For this test, the tree was located next to a building at the University of Southern Queensland. A photograph of this tree is shown in Figure 3-7(a) and the output voltage obtained is shown in Figure 3-7(b). The output voltage hovered around 1.57 V and the signal dropped at the second 718 because the tree leaves were moving slightly and allowing the sun light to reach the ESJ. As seen in Figure 3-7(b), the output voltage is higher than the output voltage observed under the light tree shade condition. This shows the ability of the ESJ to record the effective shade density that users are in.

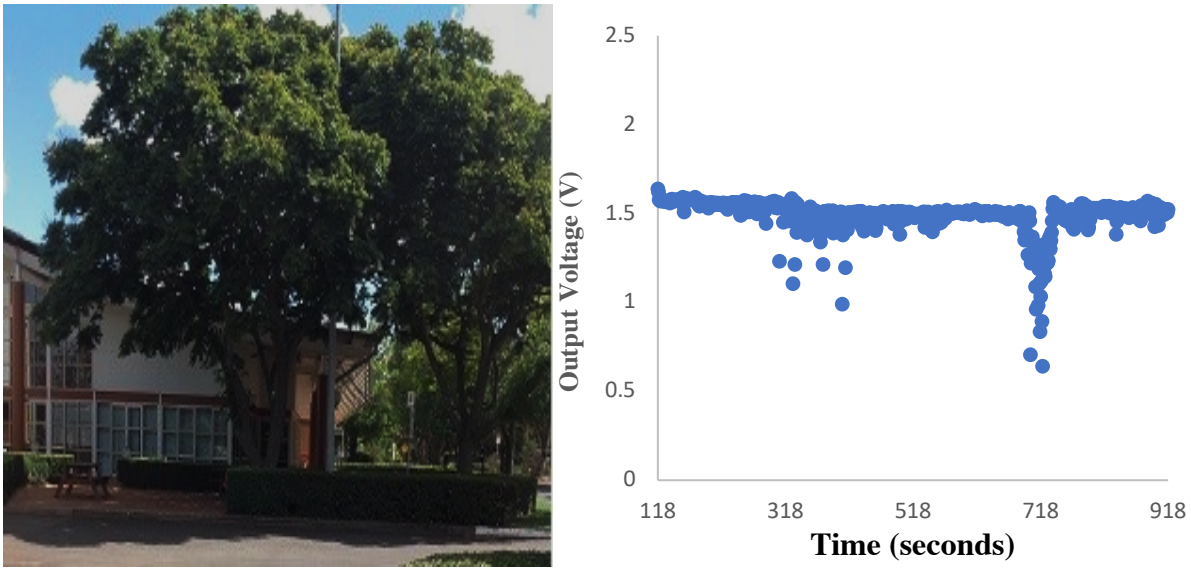

(a) (b)

Figure 3-7: (a) Heavy tree shade at the University of Southern Queensland, (b) Output voltage of the ESJ in the heavy tree shade location.

3.4.5 Fixed shade structure

A shade structure in a garden next to the University of Southern Queensland was chosen for fifth static environment test, as shown in Figure 3-8(a). The output voltage of ESJ under this shade structure is shown in Figure 3-8(b). The resulting voltage is around 2.3 V from the start to 450 seconds, after which the voltage dropped to zero. The dropping in the signal occurred as the ESJ (placed on the table under the shade structure) was exposed to direct sunlight. The ESJ was shaded until the sunlight reached the surface of the ESJ from the side of the shade structure. There are two readings of the voltage at the seconds of 667 and 668; these are not zero and have values of 1.136 V and 2.38 V respectively. This occurred because there were people under the shade structure on the day of experiment and one of them crossed in the front of the ESJ and this resulted in some shade reaching the photodiode.

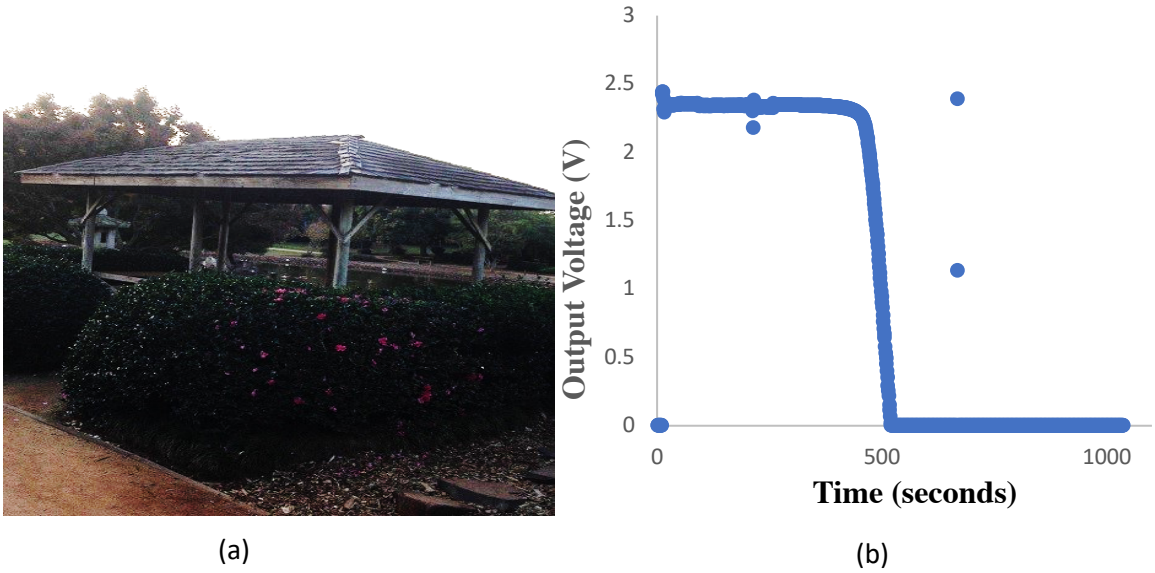

Figure 3-8: (a) A shade structure located in a garden next to the University of Southern Queensland, (b) ESJ output voltage under the shade structure.

3.4.6 North facing verandah

The sixth static environment was a north-facing verandah of building at the University of Southern Queensland this is shown in Figure 3-9(a). The output voltage of the ESJ at this verandah is shown in Figure 3-9(b). As it can be seen the output voltage, the verandah provided more shade than either the heavy tree or light tree; the output voltage was only slightly less than the full shade condition output voltage. An increase in the output voltage at the count 200 was also observed. This occurred because a person crossed in the front of the ESJ during the test.

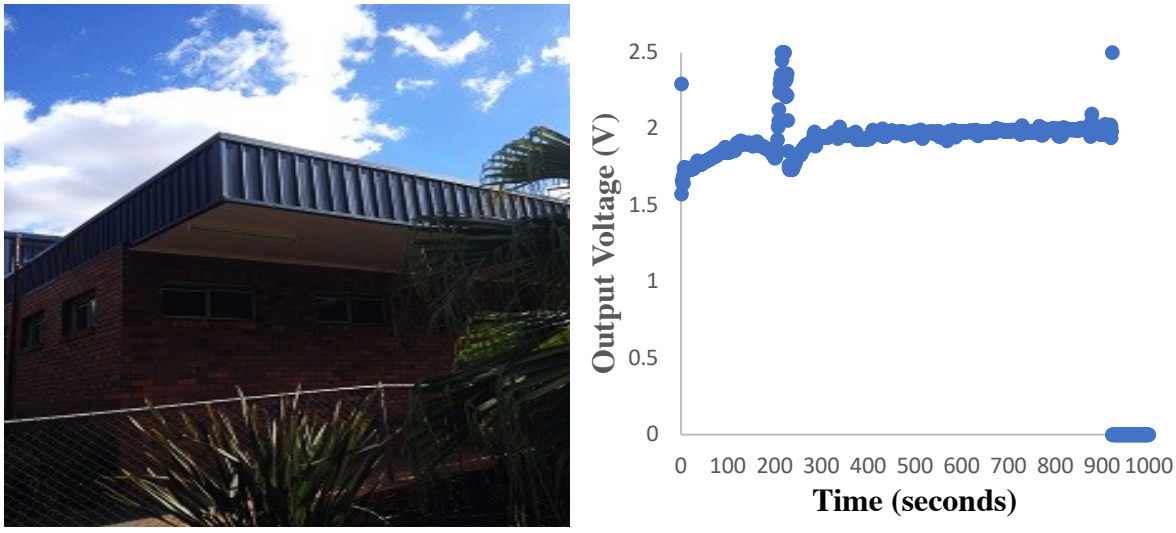

(a) (b)

Figure 3-9: (a) The north facing verandah of building at the University of Southern Queensland, (b) The output voltage of ESJ in the verandah.

Figure 3-10 compares the influence of shade provided by three static environments: a fixed shade structure (black line), light tree shade (red line) and heavy tree shade (blue line). Fixed structures, such as verandahs, awnings and purpose-built shade covers, provide a constant level of shade protection, resulting in a constant ESJ output as is evident in Figure 3-10 (upper dark line). For trees and natural vegetation, movement of canopy leaves and branches produce noticeable fluctuations in the diode output voltage. For the tree that provided the least level of shade protection, the changing orientation of the shade pattern with respect to the movement of the solar disc is also evident in the steady increase in the monitored output voltage, indicating an increase in shade density (bottom red line in Figure 3-10).

The above tests having demonstrated the capacity of the ESJ for detecting different types of environments, several 'walk around' tests were conducted to demonstrate that personal exposure patterns could be detected, and UV exposures estimated from ambient broadband radiometers. These tests showed primarily 3 things: i) periods indoors, ii) periods in open environments, and iii) periods protected by shade.

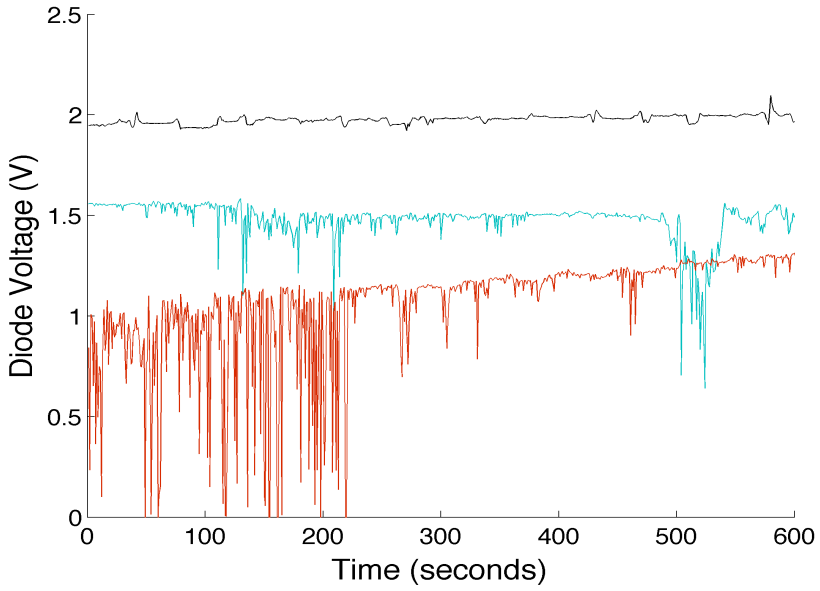

Figure 3-10: Compression of ESJ output monitored in different static environments (Black - shade structure; blue - dense tree shade; red - light tree shade).

3.5 UV Dose Estimate Field Trials

In order to show the ability of the ESJ to classify the type of environment experienced outdoors, a series of walking tests were conducted in 5 trials, where the ESJ was walked to at least 4 different stations during each field test. Trials were held in different times of the day and for around 2 hours each.

3.5.1 Trial 1

The first exposure trial was conducted on 22 September 2016 and involved holding the prototype ESJ board with the PMA2100 radiometer close to a horizontal plane at waist level while walking continuously to and from 4 different locations and staying for 30 minutes in each location.

The trial started in an open sun environment between 1:25 pm and 1:51 pm. Then, the ESJ was then carried to the second location, which is light tree shade. The ESJ was placed under the tree for another 30 minutes between 1:57 pm and 2:23 pm. The day of the measurement was slightly windy and cloudy. At 2:23 pm, the ESJ was carried to the third location (number 3 on the map in Figure 3-11) which is the area between blocks C and D at the University of Southern Queensland. This area is heavily shaded by large trees. After that, at 2: 53 pm, the ESJ was carried to the fourth location (number 4 on the map in Figure 3-11), which was indoors (full shade) inside Block C and measurements were taken until 3:25 pm.

Figure 3-11: Toowoomba campus map showing the locations of the first walking trial, starting with (1) full sun, (2) light tree shade, (3) shaded area with heavy trees between blocks, and (4) full shade.

The output voltage of the ESJ for the first walking trial is shown in Figure 3-12 below. The signal obtained is divided into 4 sections in Figure 3-12, where each section describes the output voltage of ESJ at each location. Patterns in personal exposure are also shown for trials 2, 3, 4 and 5.

The difference in the output voltage produced by varying the type of environment is clearly visible. The output voltage can also be observed to vary with change in the shade density. As seen in Figure 3-12, section 1 indicates the output voltage for the first 30 minutes in full sun. The signal obtained in this period is a straight line at 0 V. In section 2, Figure 3-12, the output voltage signal had some falls and spikes, with this observation reflecting that the measurement was under light tree shade where sunlight passes through the tree's leaves to the ESJ photodiode surface. The weather was also slightly windy, so the leaves were moving and allowing the light reaching the diode to fluctuate. This period was followed by a few minutes' walk until the ESJ was set in location 3. In section 3, the output voltage signal has some drops and spikes too, however the output voltage is higher than that in section 2 because there was more shade in the

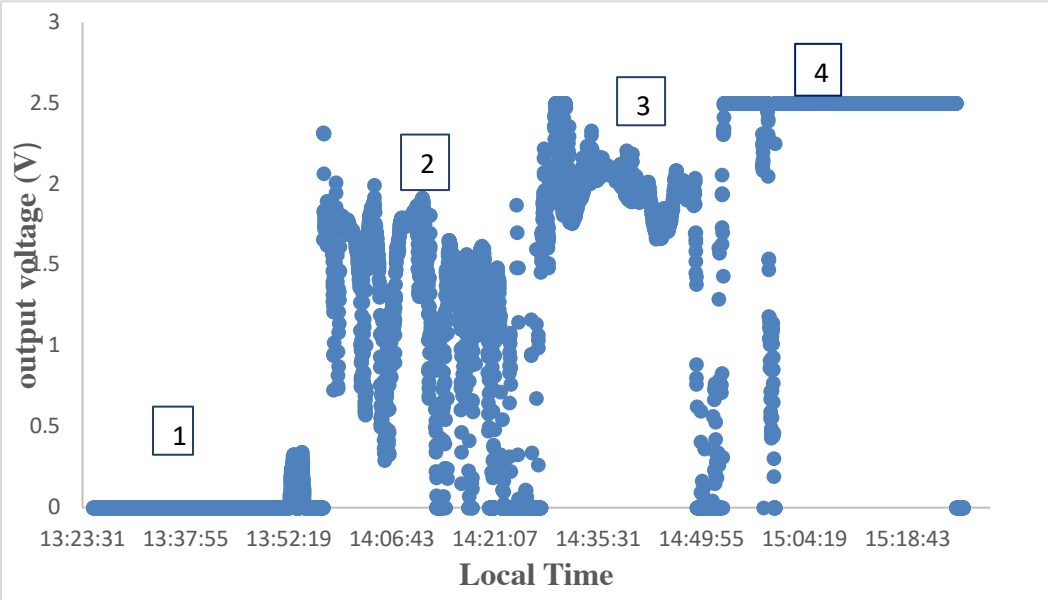

Figure 3-12: ESJ output voltage measured from 1:25 pm to 3: 25 pm on 22 September 2016.

third location of this trial. Section 4 is the output voltage of the ESJ for 30 minutes' measurement in full shade. The obtained signal is a straight line at 2.5 V.

3.5.2 Trial 2

The second field exposure trial was undertaken on 24 September 2016 and started at 11:40 am. During this trial, 4 locations were visited, starting with exposure to full sun (no shade location). This location was in the front of Block R (University of Southern Queensland Library). The ESJ was then moved to the second location where there was light tree shade. Sunlight measurements were recorded there between 12:10 pm and 12:40 pm. After that, the ESJ was moved to the third location (an area under between two very large trees which provided dense shade). The ESJ remained there from 12:40 pm to 1:10 pm before finally being walked to the last location (indoors) and remaining there from 1:10 pm to 1:40 pm. The distance between the 4 locations is very short as shown in the map in Figure 3-13.

Figure 3-13: Toowoomba Campus map showing the locations of the second walking trial starting with (1) full sun, (2) light tree shade, (3) in between two heavy trees and finally in (4) full shade.

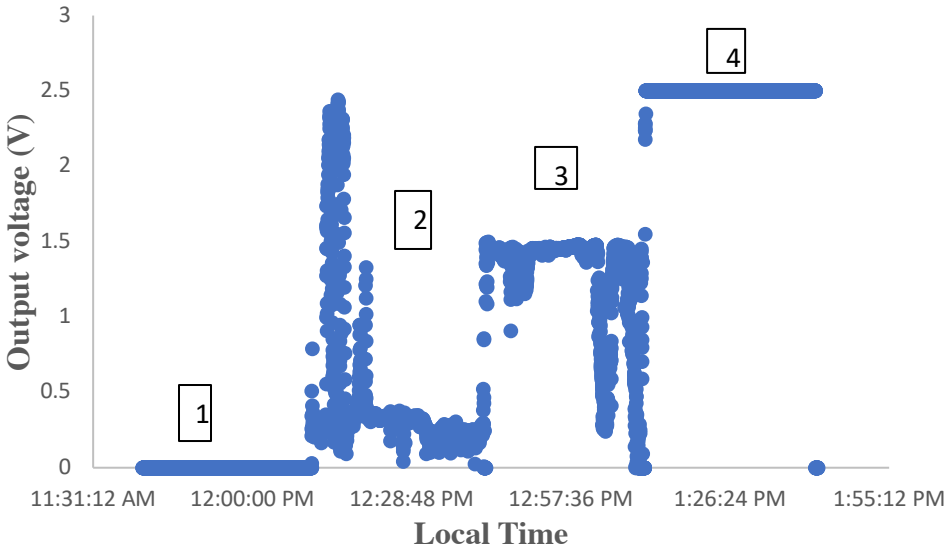

Figure 3-14: ESJ output voltage measured between 11:40 am and 1:40 pm 24 September 2016.

The output voltage of the ESJ of the third field trial is shown in Figure 3-14. It clearly shows the difference between the environments of the 4 locations in terms of shade. The output voltage of the ESJ between 11:40 am and 12:10 pm at first location (full sun) is shown in section number 1. The output is a straight line at 0 V. The distance between the first location and the second location was very short (taking around one minute to traverse). The output voltage of ESJ under light tree shade is shown in Figure 3-14 section 2. In this section, there is an increase observed in the signal at 12:14 pm, 12:15 pm and 12:20 pm. This occurs because of increasing shade caused by the movement of tree leaves as there was some wind on the day of measurement. Section 3 in Figure 3-14 gives the output voltage of the ESJ for 30 minutes at the third location (the area between two trees which provided dense shade). As can be seen in section 3, there are some drops in the signal at 1:03 pm and 1:10 pm. These were again caused by movement by the trees, allowing more sunlight to reach the ESJ's surface, leading to a decrease in the output voltage. The output voltage is higher than it is in section 2 because the shade quality had increased. In the final step of this trial, the ESJ was moved to the fourth location, which was indoors for a period of 30 minutes. The output voltage is shown in section

4 in Figure 3-14. Here, the output voltage is consistently 2.5 V. It is shown clearly that the improvement in the quality of shade from section 1 to section 4 in Figure 3-14, is reflected in output voltage increases and increased consistency.

3.5.3 Trial 3

The third field exposure trial was conducted on 24 September 2016 and involved visiting 4 different locations, starting measurement at the first location, which was inside Block R (indoors) at the University of Southern Queensland. The trial began at this location from 2:00 pm to 2:30 pm. The ESJ then was moved to the second location, which was a verandah of Block Y. The ESJ remained there between 2:32 pm and 3:02 pm, before moving to a third location (light tree shade) and remaining there between 3:02 pm and 3:32 pm. The ESJ was then moved to the last location which was open to the sun (no shade) where measurements were taken from 3:32 pm to 4:02 pm. Then the ESJ circuit was switched off and the radiometer reading was recorded at the same time (Table 3-2).

Figure 3-16 shows the output voltage of the ESJ during the third field trial. The 4 sections in Figure 3-15 show the output voltage of the ESJ in different types of locations, where the signal

Figure 3-15: Toowoomba campus map showing the locations of the third walking trial starting with (1) full shade, (2) verandah, (3) light tree shade and (4) full sun

reflects the type of shade. The shade in section 1 was complete (indoors), as shown by the consistent high signal that is a straight line. In section 2, the signal is not consistent as the signal was also affected by light tree shade, as trees were in the front of the verandah of Block Y. As seen in Figure 3-15, there are some drops in the signal between sections 1 and 2. This occurred because of the walk for 2 minutes between different types of environments, including full sun and shade. In section 3 of Figure 3-15, there is periodic increase in the voltage signal as the leaves shade the photodiode and at other times the signal drops to 0 V. Here the tree is very light shade, so the sunlight predominately passes through the leaves before reaching the ESJ sensor. In section 4, Figure 3-15, the signal falls to 0 V as the photodiode was placed in a full sun environment. The movement from location 3 to 4 was very brief as the locations are very close.

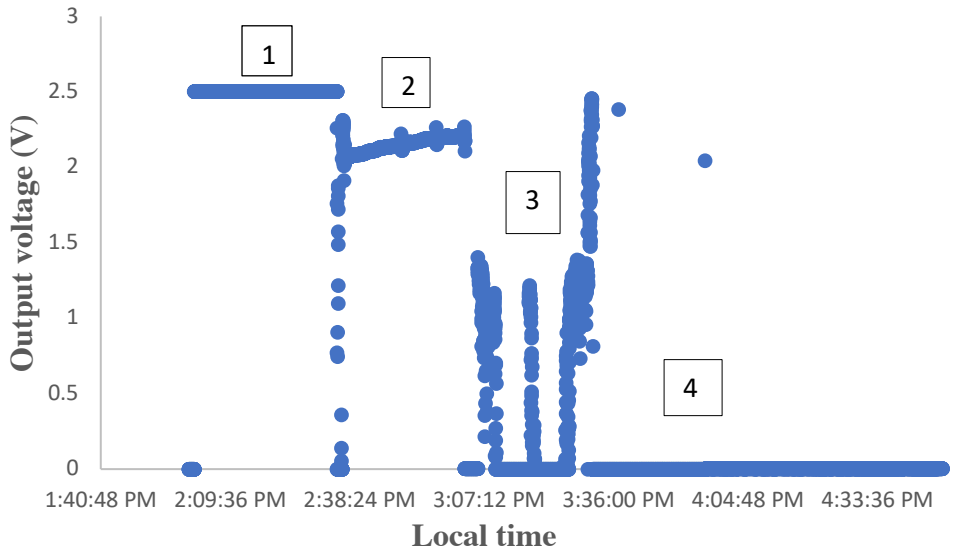

Figure 3-16: ESJ output voltage measured between 2:00 pm and 4:02 pm on 24 September 2016.

3.5.4 Trial 4

The fourth field exposure trial was undertaken on 26 September 2016 during the afternoon and involved walking through 4 different locations, starting with the first location (indoor, station (1) shown on the map in Figure 3-17) inside Block D for a 30 minute period between 1:00 pm and 1:30 pm before moving to a verandah in Block R (station 2) for the period between 1:33 pm and 2:05 pm. After that, the ESJ was carried to very light tree shade next to Block Z (station 3) between 2:12 pm and 2:35 pm before being moved to the last location (station 4) which was exposed to full sun until 3:05 pm. At 3:05 pm, the ESJ circuit was turned off and radiometer reading was recorded.

Figure 3-17: Toowoomba campus map showing the locations of the fourth walking trial, starting with (1) indoor(full sun), (2) verandah, (3) light tree shade, and (4) full sun.

Figure 3-18 below shows the output voltage of the ESJ of the fourth walking trial. In section 1, the output voltage is consistent because the environment was located indoors. In section 2, the environment was a verandah; however, direct sunlight reached the ESJ photodiode and therefore shows a similar result to full sun. The signal at this stage has some intermittent spikes because occasionally people crossed in front of the photodiode during the measurement.

Section 3 in Figure 3-18 shows the output voltage of the ESJ under very light tree shade. Under this condition, the output voltage was 0 V as direct sunlight often reached the photodiode. In section 4 of the figure, the output voltage is 0 V as the measurement in this section was taken in a full sun environment. This trial recorded the highest exposure of all 5 trials. This is clearly seen in Figure 3-18 (sections 2, 3, 4) because of the minimal shade experienced during the test in the last three locations, which were often exposed to the sun.

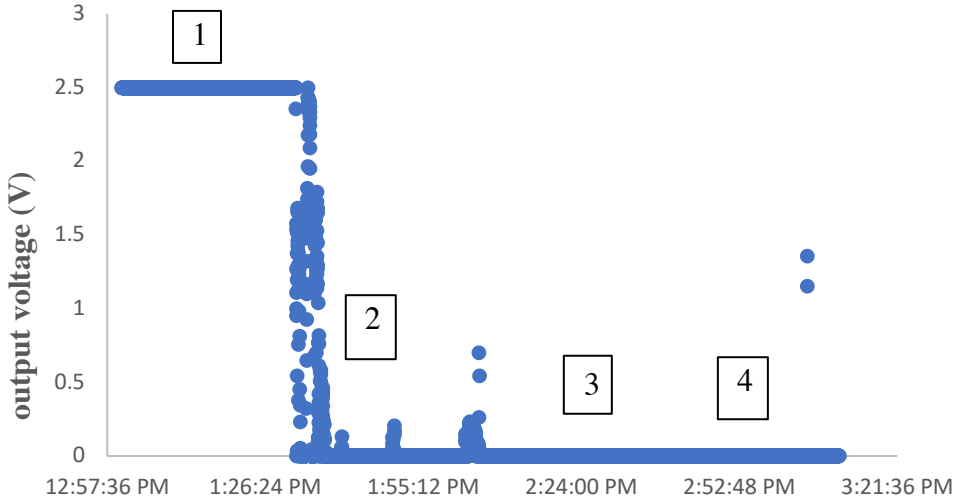

Figure 3-18: ESJ output voltage measured between 1:00 pm and 3:05 pm on 26 September 2016.

3.5.5 Trial 5

The fifth field exposure trial was undertaken on 27 September 2016. This time, the trial started at 11:45 am to 12:15 pm in a full shade location (inside Block C, station 1, Figure 3-19). The ESJ was then moved to heavy tree shade opposite Block Z (station 2, Figure 3-19) where it remained between 12:27 pm and 12:57 pm. Following this exposure, the ESJ was moved to light tree shade behind Block Z between 1 pm and 1:30 pm (station 3, Figure 3-19). After that, the ESJ was moved into the open sun (station 4, Figure 3-19) between 1:30 pm and 2:00 pm in an area opposite the Japanese Garden Gate. Then the ESJ circuit was switched off and the radiometer reading was recorded.

Figure 3-20 shows the output voltage of the ESJ during the fifth trial. The output signal is

Figure 3-19: Toowoomba campus map showing the locations of the fifth walking trial starting with (1) full shade, (2) heavy tree shade, (3) light tree shade, and (4) full sun.

divided into 4 sections. Section 1 represents the output voltage of the ESJ in a full shade environment (the first location of this trial). Again, the signal obtained is consistently 2.5 V. As has been noted in Figure 3-20, there are some drops and spikes in the signal between section 1 and 2. This is because of the long walk between the first and second locations. During this walk, different types of environments have been passed through, such as full sun, shade structure and full shade. In section 2 of Figure 3-20, the output voltage of the ESJ is shown for 30 minutes under very heavy tree shade. High signal spike fluctuation between 2.5 V and 0 V appear in the signal between sections 2 and 3 as the ESJ was moved between these environments due to walking in full shade and full sun environments. Section 3 shows the output voltage of the ESJ under very light tree shade. Signal spikes in the ESJ output occur in this section because of the movement of tree leaves during the measurement. The output voltage of the ESJ for the measurement in the last location (full sun) is shown in section 4.

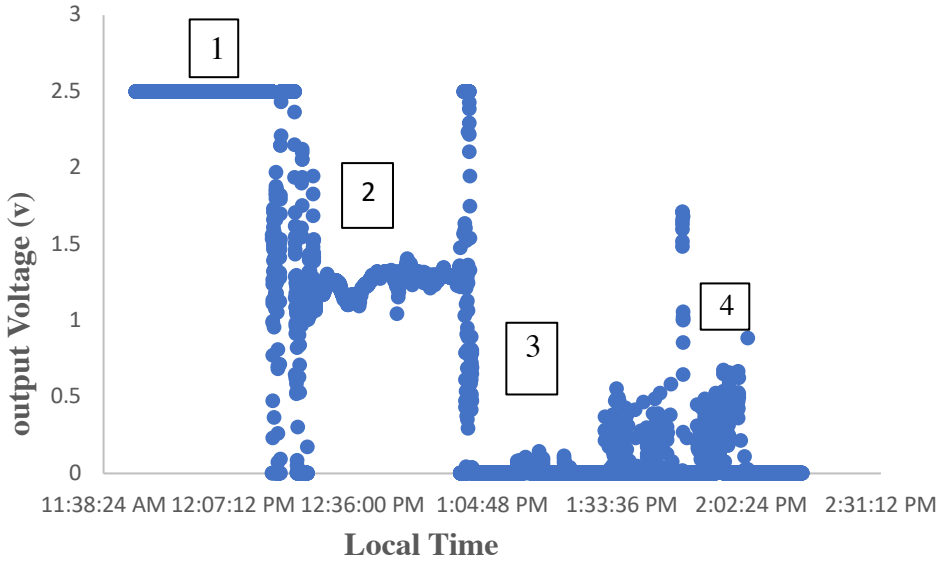

Figure 3-20: ESJ output voltage measured between 11:45 am and 2:00 pm on 27 September 2016.

Significant spikes appear in the signal because of the movement of the people crossing in the front of the ESJ during the measurement.

3.5.6 Field Trial summary

Table 3-2: Starting and finishing times, dates and measured simultaneous UV exposure recorded by the PMA2100 during each field trial.

Trial Number	Starting Time	Finishing Time	Dates	UV exposure
Trial 1	1:25 pm	3:25 pm	22/09/2016	179 J/m^2
Trial 2	11:40 pm	1:40 pm	24/9/2016	506 J/m^2
Trial 3	2:00 pm	4:02 pm	24/9/2016	135 J/m^2
Trial 4	1:00 pm	3:05 pm	26/9/2016	341 J/m^2
Trial 5	11:45 am	2:00 pm	27/9/2016	531 J/m^2

3.6 Estimate of UV Field Exposure

The environmental tests presented above have shown the ability of the ESJ to monitor personal exposure patterns. In this section, the results of employing the ESJ to record periods of outdoor activity for estimation of UV exposure with ambient radiometers will be outlined.

Table 3-3 compares ESJ exposure estimates with PMA2100 radiometer measurements for each field trial conducted in September 2016. Minimum and maximum ESJ exposure limits were determined using the methodology of section 2-8 for each of 5 separate field trials ranging in personal exposures estimates of between 207 and 811 $\mathrm{J/m^2}$. The relative error, *RE* (Equation 3.1), describes the variance between the ESJ UV exposure estimates and the measured PMA2100 UV exposures. $E_{PMA2100}$ recorded simultaneously during each trial, where:

$$RE = 100(E_{est} - E_{PMA2100})/E_{PMA2100} \qquad (3.1)$$

Table 3-3: Comparison of erythemally effective field exposure (PMA2100, solar light Co.) to ESJ UV exposure estimates (USQ global 501 biometer, Solar Light Co.). %RE represents the relative error of the ESJ UV exposure estimates relative to the PMA2100.

Trial number	PMA2100 Radiometer (% of Ambient)	ESJ exposure estimate. ($\mathrm{J/m^2}$)	RE (%)
Trial 1	179 (31%)	313	+75
Trial 2	506 (36%)	853	+69
Trial 3	135 (23%)	207	+53
Trial 4	341 (37%)	589	+73
Trial 5	531 (37%)	811	+53

The results show that for the field trial series, comparing outdoor exposure time to ambient meters has a tendency to over-predict the actual personal exposure. The ESJ as developed does,

however, provide a reasonable estimate of the sunlight conditions experienced as an individual moves between indoor, outdoor, and shade environments.

Chapter 4: Discussion

The main purpose of this project is to develop a cost-effective personal electronic sun journal (ESJ). The ESJ is built from inexpensive readily available infrared photodiode technology; this photodiode measures personal sun exposure patterns. The ESJ can be used to complement traditional UV dosimeters that measure total biologically effective exposure by providing a time-stamped sun exposure record.

4.1 Research Goals of this Project

The research goals of this project are:

1. To develop a new personal electronic sun journal (ESJ), employing an inexpensive infrared photodiode;
2. To test the traditional infrared photodiode to determine if it can be utilised as a personal electronic sun journal for characterising personal sun exposure patterns; and
3. To replace paper-based journals (self-reported volunteer recall) to complement existing exposure monitoring in UV research studies for estimating periods of exposure and personal exposure patterns.
4. To determine personal patterns and time spent in three state: (1) indoor conditions, (2) full sunlight conditions, and (3) semi-shaded environments.

4.2 Development of a Novel Personal Exposure Pattern Monitor (Electronic Sun Journal)

The developed ESJ is manufactured from a low power circuit consisting of a 3 V battery, a 20 kΩ resistor, a BPV22F infrared photodiode and a data logger. The designed circuit, presented as a prototype in this research, has some limitations (such as the size of the ESJ which was tested using a developmental electronic bread-board). This being the case, the circuit was carried in a horizontal orientation while personal exposure measurements were taken during the experimental work. Due to the simplicity of the circuit design, future versions of the ESJ will be significantly more compact and may include lapel or wrist band variants. The general design, however, has the advantage of cost-effectiveness over existing UV electronic dosimeters (the total cost of the designed ESJ circuit is shown in Table 4-1), as the infrared photodiode is a cost-effective and readily available photodiode.

The photodiode employed in the designed circuit to monitor exposure patterns was shown to be capable of providing sufficiently high temporal resolution data on behavioural exposure patterns measured during the experimental work of this project. Such high-resolution exposure data cannot be obtained by using traditional self-reported sun diaries. By employing an ESJ to replace paper sun diaries, high electronic sampling rates have the potential to improve the accuracy of long-term epidemiological cumulative exposure studies. This data can also be reduced to provide daily, monthly or longer-term personal sun exposure records where exposures measured by a UV radiometer can be integrated over the outdoor exposure time record measured by the ESJ.

Published exposure ratio measurements, which express measured ambient UV relative to any given body site for a range of human activities, including, walking, sitting, kneeling etc, can be used to provide holistic estimates of UV exposure. This represents an advantage over wristband, or lapel

worn electronic UV dosimeters which provide a record of exposure to a specific site on the body. The ESJ offers significant advantages in terms of cost effectiveness as the components can be readily sourced due to the high abundance of IR diodes on the market. Furthermore, an ESJ built using an IR photodiode does not require signal amplification as IR in an outdoor environment is several orders of magnitude higher than the available UVB. This, and the low cost of IR photodiodes highlights the potential for ESJs to be used in research applications where the number of subjects to be studied is large. Provided a suitable datalogger can be coupled with an ESJ, the costs of producing a set of working prototypes for application in research can be kept low.

Table 4-1: Approximate costs of the designed circuit component in USD.

Component	Approximate cost (USD)
PBV22F infrared photodiode	$1.24
2 x 10 KΩ resistance	$0.34
3V coin cell battery	$1.41
3V battery holder	$0.92
TK-4703 data logger	$213.00

The data logger employed in this project is a portable data logger (Tinytag Talk 2 voltage data logger (TK-4703)). The TK-4703 measured voltage input between 0 and 2.5 V. This is the same output range of the Photodiode divider circuit (See Figure 2-2). It was the most expensive part of the designed circuit; however, cheaper data loggers are also compatible with this circuit. These may include smartphone loggers, miniaturised computers, and SD card systems. Any readily available data logger can be connected to the developed ESJ circuit. This includes, for example, smart phone memory or data loggers similar to those found in commercially available fitness

trackers. An 8-bit (1 byte) digital logger can store up to 256 distinct voltage levels in the 0–2.5 V range for each byte of available memory. Thus, a system developed using 1 megabyte of free memory could store up to 1,048,576 million data samples. At a sample resolution of 1 second, even this moderate memory capacity would allow storage over 12 continuous days.

The TK-4703 data logger used in this project required no external assembly and included data download and control software. The logger was commercially available and had a memory capacity of 16 kilobytes, so it could sample sun exposures in second long intervals for a period of 4.5 hours. This provides an advantage to the developed ESJ over a paper-based sun diary by recording accurate high-resolution data for a long period. Another advantage of the data logger employed in the developed ESJ is that it can be set to log signal voltages over variable time periods as desired, extending the range over which the ESJ can be used. The length of time the ESJ can record depends on the memory capacity of the logger used. Commercially available UV electronic dosimeters employ greater memory capacity. UV electronic dosimeters such as the Scienterra (2019) range sell for approximately $450 each, thus the developed ESJ, including the TK-4703 used in this project is approximately half the cost of a commercially available dosimeter. In this project, the research objective is not to redevelop a cost effective datalogger, therefore a working data logger has been implemented in the ESJ prototype that was used for testing in different environments.

As mentioned earlier, the designed ESJ utilises a low power 3 V battery source. This battery was employed during all the tests undertaken in this project, including preliminary development, exceeding 20 hours of continuous operation. It has been estimated that the designed ESJ with the components presented in Table 1 above could run continuously for several weeks (during data collection) without the need for a battery change. The power to the TK-4703 datalogger is

independent of the circuit as designed and only required for computer communication and data download. Any power needed at this stage would be obtained by using the charger connected to the TK-4703 or computer USB communication functions.

4.3 Testing of the Electronic Sun Journal

The prototype ESJ (Figure 2-8) was tested initially in both an indoor and outdoor environment. The output voltage obtained fell to 0 V when placed outdoors or in full sun. When exposed indoors under ordinary indoor lighting, the monitored voltages reached a maximum of 2.5 V. This is the equivalent voltage for exposure in full shade. This initial result showed that the design operated correctly in this project.

After confirming the correct operation of the ESJ circuit, a cosine response test was performed because it was important for the infrared photodiode to have a good cosine response to ensure that the ESJ measurements reflect the realistic exposure patterns for its users. During the development of the ESJ, the BPV22F photodiode (Vishay semiconductors) was selected as the best photodiode, as it has a good cosine response (based on its manufacturer's data sheet). The photodiode manufacturer data shows that its cosine response matches the natural cosine response between 0° to 80°. The cosine response test is performed to characterise the ESJ with respect to the manufacturer's specifications. When the cosine test was performed in the laboratory at the University of Southern Queensland, the result obtained showed that the measured ESJ response up to 40° deviates by no more than 13% of the normal cosine ratio, slightly underestimating the normal cosine response for angles greater than 40° and overestimating the normal cosine response for the angles less than 40°. This occurred due to the inaccuracy of the equipment in the lab, in particular the affixing of the ESJ circuit onto the stand holder in the front of the incident infrared

source. The ESJ circuit was not stabilised on the holder at exactly 0° incidence, so it was hard to know whether the incident light was perfectly perpendicular to the photodiode surface. The ESJ circuit attached to this assembly was rotated through 10° increments to measure the cosine response in situ. A diffuser was not fitted to the BPV22F photodiode in this project, as the ESJ measures the amount of shade not the exposure. For designs utilising different infrared diodes, the use of a diffuser to approximate the natural cosine response is recommended. In a future study the point of housing as a large determinant of good cosine response could be investigated.

The circuit response with ambient temperature was tested under controlled laboratory conditions to ensure consistency in signal output during winter versus summertime use of the ESJ. To determine this response, the ESJ was placed within 10 cm of a glass-filtered heating lamp. The glass filter reduced the circuit response to below the maximum output of 2.5 to 2.3 V. The reduction in signal voltage ensured either a positive or negative change in output voltage could be monitored with increasing temperature. The output voltage (Figure 3-3) was monitored using an oscilloscope, as the circuit was heated by a hair dryer unit from 16° to 60°C. The temperature coefficient of the circuit monitored under these conditions was measured to be -0.01 V/°C and exceeded the characteristics stated by the manufacturer. This may be because of the limited range of the temperature which the BPV22F photodiode was tested in the lab (10° to 60°C) as the ambient temperature could not be increased or decreased to beyond this range. The reduction in the measured signal voltage with expected changes in ambient air temperature when used to monitor sunlight levels in the field is, therefore, negligible compared with the full signal range of the ESJ which is capable of logging an 8-bit output from 0 to 2.5 V.

After ensuring that the ESJ could be employed in normal summer and winter temperatures, the ESJ signal response was tested with changing sky view. A sky view test was completed in late

spring (16 November 2016). For this test, the BPV22F photodiode response was measured with increasing diffuse solar radiation exposure. Specifically, to determine the photodiode sensitivity to shaded outdoor exposure conditions, the test was performed in the open air using a shadow shield attached to a vertically upright stand assembly that was moved above the surface of the photodiode during cloud-free midday conditions. The tested height range for the shadow shield equated to an approximate range in a shaded sky view of from 0 to 99.8% measured over 21 steps. The output voltage of the ESJ obtained relative to the sky view (Figure 3-2) showed that the output voltage falls rapidly to 0 V, whenever the sky view approaches 100%. Therefore, any monitored ESJ readings greater than 0 V are known to be due to either exposure to diffuse solar radiation in an open environment or a combination of direct and diffuse (global) solar radiation.

It was important to test the developed ESJ indoors and outdoors to ensure its ability to classify the type of environment typically occupied by users. To operate effectively, the ESJ was tested to determine if it could detect direct sun, shaded environments and several types of partially shaded environments. These included full shade, heavy tree shade, light tree shade, shade under a building verandah and a shade structure. For these tests, the ESJ circuit was placed in a stationary position in each of the environments presented for a period of at least 15 minutes. Characteristic of each tested environment was the increased output voltage of the ESJ with increasing shade density (reduced sky view). The output voltage of the ESJ in each static environment as shown in Chapter 3 (Figure 3-4b, Figure 3-5b, Figure 3-6b, Figure 3-7b, Figure 3-8b and Figure 3-9b), reflects the type of shade in that environment. In the condition of a full shade environment, the ESJ output voltage when plotted against time showed a straight line consistently occurring at 2.5 V. However, in the condition of an open environment with no shade, the output voltage versus time was consistently 0 V. Output voltages for the partially-shaded environments (including light and heavy

tree shade), the shade structure and a building verandah, showed fluctuations in signal voltage between 0 V and 2.5 V. These results demonstrated the ability of the ESJ to determine and classify the type of environment (in terms of shade) where the users were located. A comparison between the output voltage of the ESJ in static shaded environments was plotted in Figure 3-10. This figure showed clearly the influence of shade provided by a fixed shade structure compared with trees and natural vegetation. For fixed structures, such as verandahs, awnings, and the purpose-built shade structure, a consistent level of shade protection at a constant SZA resulted in a constant ESJ output, as was evident in the output voltage comparison for the three environments. For trees and natural vegetation, movement of the canopy leaves and branches produced noticeable fluctuations in the output response voltage. For the tree that provided the least level of shade protection, the changing orientation of the shade pattern with respect to the movement of the solar disc (changing SZA) was evident in the steady increase in the monitored output voltage. Therefore, it was shown that the qualitative level of shade protection can be approximated by ESJ voltage for an individual monitored in a stationary condition under the shade of a tree or static structure where the shape of the obtained signal would define the type of shade. For example, if the signal is a straight line with 2.5 V, this means the type of shade is indoor (full shade). A fluctuating signal is indicative of tree shade or movement of the individual. This is a significant outcome as it shows that the ESJ can be used to monitor not only personal exposure times in full sun and indoor environments but can also give an indication of the periods of time when a user may be utilising partially shaded environments.

4.3.1 Environment limitations

When the infrared ESJ is placed behind glass, or windows of a building, the recorded exposure reading will be positive. Thus, it may be possible to get a false impression that a user may be

outdoors, when actually partially protected by an indoor environment. Glass is an effective absorber of UVB radiation but will generally transmit UVA and near infrared wavelengths in the absence of varied glazing techniques or protective tinting. Thus, the ESJ would record personal exposures near large window frames or greenhouses, for example. This is a limitation to be considered should future users of the ESJ be regularly working behind glass. This may affect studies where biologically effective exposure patterns sensitive to short UVB wavelengths, including erythema, vitamin D, and some conditions of the eye (such as photokeratitis) need to be examined.

The ESJ as designed and tested in this research is not waterproof. Future implementation of an infrared ESJ for monitoring personal sun exposure behaviour could be built into weather resistant (or submersible) housings, provided the infrared photodiode sensor remains unobstructed and exposed to the environment.

The developed ESJ is not sensitive enough to detect changes in cloud, aerosol, dust or significant variation in solar elevation. A similar IR diode system could be developed in the future that is much more sensitive with a higher resolution data logger (16 or 32 bit) and be investigated with appropriate filters.

The ESJ has not been tested around geography with high UV reflectance, such as water, snow or sand environments as it is designed to be used primarily in urban and school working environments. High UV reflectance does not affect the ESJ result as it is designed to measure the exposure patterns by determining the amount of shade.

4.3.2 In situ testing

The field results obtained for the ESJ in different types of environment showed the ability of the ESJ to detect direct sun, shaded environments and partially shaded environments. The ESJ could classify periods in partially shaded environments, such as tree shade, in addition to being able to classify the type of tree shade (heavy or light). On that basis, dynamic exposure tests were undertaken to determine if the ESJ could accurately classify exposure of an individual to periods of indoor exposure, periods within a shaded environment, and periods in direct sun. These tests confirmed that the ESJ can be used by individuals during their daily routine to detect their exposure patterns to sunlight. This would be useful for many studies that aim to explore personal exposure behaviour.

A total of five outdoor exposure pattern trials were conducted at the University of Southern Queensland. Each trial studied the ESJ signal pattern in four different environments, one of them was indoors (full shade) and three were outdoor environments offering varying levels of shade protection. Trials were held at various times of day for periods between two to three hours under different ambient conditions, including clear sky and cloud-affected periods. All trials were conducted by walking the ESJ, held and maintained in a horizontal plane in the palm of the hand, to and from at least three separate locations on campus. These locations often included environments between building structures, heavy and light tree shade, various shade structures, and open outdoor environments. The results of the trials showed that there are clear periods of exposure to open and shaded outdoor environments. Indoor environments show the saturated condition of the ESJ at 2.5 V while environments in full sun recorded a signal of 0 V. The results obtained prove that, when the ESJ is worn on an exposed surface of the body, the ESJ can provide quantitative information of an individual's day to day sun exposure pattern.

These tests also show that when the ESJ is employed for use as a practical cost-effective high-temporal resolution sun journal, the infrared photodiode provides sufficient information on the ambient environment. The ESJ provides details on behavioural exposure patterns not able to be recorded to such high resolution using traditional self-reported paper sun diaries. High sampling rates have the potential to improve the accuracy of long-term epidemiological cumulative exposure studies. They also enable precise measurement of intermittent or incidental sun exposure patterns while removing the burden placed on study participants to recall past exposure behaviour. High-temporal resolution exposure pattern data may be beneficial to studies that seek to determine shade use in school playgrounds, public spaces or the working environment. It may also be useful for determining exposure patterns in different professions. Being a cost-effective alternative to existing electronic UV dosimeters, which employ AlgaN photodiodes, the ESJ could be utilised in studies to detect patterns of exposure behaviour that involve large numbers of participants.

4.4 Approximating Personal Ultraviolet Exposure

The developed ESJ cannot be employed as a UV dosimeter as the ESJ does not have the ability to monitor personal UV exposure dose. Approximations were, however, made by comparing noted periods of time outdoors with ambient UV radiometers located in proximity to the ESJ user. These results were variable but demonstrate the potential of the ESJ as a proxy instrument for estimating personal UV dose.

The designed ESJ can give some general indication of personal exposure if the ESJ is used near an ambient UV meter. In this project, UV exposure estimates obtained by weighing periods of known personal sun exposure in unprotected or partially shaded environments to a calibrated ambient UV radiometer were validated against the simultaneous measurement of the erythemally

effective exposure measured using the hand-held PMA2100 radiometer for each of the ESJ field trials. A global 501 UV biometer mounted on a rooftop at the University of Southern Queensland was calibrated to the PMA2100. From the September 2016 field trials, UV exposure estimates were made using the ESJ as a proxy for the ambient exposure a user is likely to be exposed to. Field trials showed that the ESJ was able to detect movement between different sunlight states, including movement into and out of full sunlight, use of shade, and indoor environments.

The technique of estimating exposure presented here may be useful if employed near any existing UV monitoring equipment such as an ARPANSA meter in Sydney, Canberra, Hobart, Adelaide, Perth, Alice Springs and Townsville (https://www.arpansa.gov.au/our-services/monitoring/ultraviolet-radiation-monitoring/ultraviolet-radiation-index). The ARPANSA radiometers provide a national network of broadband UV sensors covering most of the Australian population. Data from these and other networks is potentially under-utilised by the public. Through personal monitoring of ambient conditions, this often publicly available information can be used to make valid judgments on personal erythemally effective sun exposure habits.

The ESJ employing the use of an infrared photodiode when combined with traditional spore or film-type badges may be used to provide time-stamped information on personal exposure habits. Sun exposure pattern information, including periods of indoor, outdoor, and partially shaded exposures, would aide UV dosimeter studies that seek to determine cause and effect relationships in different population groups.

4.5 Future Directions

As infrared photodiodes are readily available, the ESJ has broad future implications. It will be useful in studies with large population groups as it can provide them with extensive data about sun exposure habits. With access to such data, future studies may be designed to help determine the cause of diseases related to sun exposure. The cost-effective infrared ESJ has the potential to greatly support studies linking UV radiation exposure to human health.

Future versions of the ESJ could be employed on a wrist-band, the vertex of a cap, or easily attached to a lapel device (although the resulted signal will be hard to analyse because of the chaos that is human behaviour and many factors would be affecting the result, however these factors would be considered in future studies). Being cost-effective, it has the potential to monitor long-term sun exposure habits, because it would provide a significant amount of data on personal sunlight exposure patterns that can be monitored without the requirement of employing a typically more expensive UV photodiode.

A large determinant of good cosine response of the ESJ is the design of the housing. However, this point could be investigated in the future study.

Filtering is not required for the sun journal results, as the fluctuations (are not noise) in the resultant signals such as light tree shade reflects the type of environment where the ESJ was placed. In terms of analysing the data obtained from the ESJ, as the users will employ the ESJ for a long period of time, and a significant amount of data will be analysed, the obtained signal may be broken down into parts based on the type of shade. For example, the signal when the ESJ is used under light tree shade is different from the signal pattern when the ESJ is used under a static shade structure. The infrared ESJ provides sufficient information in this way about personal exposure patterns of

individuals. Thus, it is possible to map personal sun exposure behaviour accurately. This would allow the development of a greater understanding of the risks faced by ESJ users in terms of their occupation, or activity (where a clear relationship is found by such research) and encourage (for example) specifically targeted health campaigns. From the output voltage signal shape, it may be known if the user is an outdoor or indoor worker. For example, office workers would likely have a different exposure pattern to construction workers as office workers spend most of their time indoors and construction workers spend more time in an outdoor environment.

The data obtained from the infrared ESJ about personal exposure habits can be used to alert individuals about their lifetime sun exposure periods. By knowing these periods, they may avoid exposure to the sun or use better sun protection strategies.

4.5.1 Interconnectivity

The developed ESJ is a prototype, consisting of an inexpensive infrared photodiode. These diodes can be integrated with existing cameras and smartphones that already utilise IR diodes. Software developed from smartphones, such as apps, could be developed to turn existing technologies into electronic sun journals, provided the existing technology has continual exposure to sunlight.

The infrared ESJ may be integrated with personal fitness monitors, providing a record of personal behaviour as well as fitness for overall health. The data could be stored on a large database of personal exposure habits able to be reviewed. This would be beneficial for studies related to personal epidemiology of sun related disease.

4.5.2 Research Implications

The signals obtained from the developed ESJ could be related to other important wavebands, such as vitamin D effective UV or erythemal effective UV, provided the potential ratio of these wavebands could be investigated at different times of the day relative to the available infrared.

The ESJ therefore has the potential to influence public health policy in relation to the health of individuals, and facilitate individuals becoming more aware of and more responsible for ameliorating their sun exposure, because using the ESJ for monitoring personal exposure patterns and estimating periods of outdoor exposure would allow individuals to be become aware of periods they spend in the sun daily.

Chapter 5: Conclusion

Excessive exposure to sunlight, especially UV radiation, causes harmful effects on human health, such as sunburn, skin cancer, eye disorders and immunosuppression. Personal sun exposure is monitored extensively in a variety of populations to ascertain the level of personal risk associated with exposure to sunlight. UV radiation dosimeters have been employed in many population groups to determine the level of personal exposure. These measurements are conducted by using either polysulphone dosimeters or, alternatively, electronic UV radiation dosimeters. However, the former is limited by requiring replacement for exposures that exceed one day, potentially increasing study costs and effort, especially for large numbers of participants; and the latter require individual calibration and are generally of higher cost.

Sun diaries have been employed in many studies to determine sun exposure. Diaries utilise questionnaires or can be used to record the time people spend exposing themselves to sunlight during their daily activity. Sun diaries have some limitations as people may have social desirability bias (people record what they think and feel, not what they really do). This research aimed to develop a novel methodology for sensing personal exposure patterns. The novel methodology involved the development of a new personal electronic sun journal (ESJ), employing an inexpensive infrared photodiode. The objective was to test the traditional infrared photodiode to determine if it could be utilised as a personal electronic sun journal, and to characterise personal UV exposure patterns. The ESJ could replace paper-based journals (self-reported volunteer recall) and complement existing sun exposure dosimeters.

This development of the ESJ was performed by testing groups of photodiodes (low cost infrared photodiodes) for their physical response. The photodiodes were chosen due to their cost effectiveness, their sensitivity to infrared radiation and their cosine response as listed by

the manufacturer. A voltage divider circuit was employed for testing the photodiodes; this circuit consisted of a 3 V battery and a resistor. In addition, a photography lamp and oscilloscope were used to measure the output voltage of the circuit under different light conditions. Each photodiode was tested in terms of maximum and minimum output voltage, temperature stability and cosine response. After the photodiodes were tested, the photodiode with the best cosine response was selected. The selected photodiode to be used in the electronic sun journal (ESJ) was a BPV22F (Vishay semiconductors). The resistor chosen in the final circuit design was 20 kΩ (this allowed detection of light levels at voltages above 0 V up to minimum light levels of just below 2.5 V). This resistor, along with the 3 V battery, BPV22F photodiode and Tinytag Talk TK-4703 voltage data logger (Germini Data loggers, UK) was used to monitor voltage. These are the final elements of the ESJ circuit.

Preliminary environmental tests were performed for the ESJ to ensure that it operated correctly and was sensitive to the environment. The ESJ was tested in two environmental conditions, including saturated exposure conditions to sunlight (full sun) and limited exposure conditions (indoors). Other tests were performed after the preliminary tests including, cosine response test, temperature stability test and sky view test. Environmental characterisation tests were then performed by placing the ESJ in different types of static environments, including an indoor environment, a north facing verandah, a fixed shade structure, light tree shade, heavy tree shade and an open environment.

5.1 Test Outcomes

Cosine response results showed that the measured response up 40° deviates by no more than 13% of the normal cosine ratio. The ESJ response, as measured using the infrared lamp and aperture assembly, underestimates the normal cosine response for angles greater than 40°.

Results of temperature stability showed that the ESJ can be employed in summer and winter temperatures that are expected to be faced by ESJ users.

Sky view results showed that when the sky view approaches 100%, the output voltage of the ESJ falls to 0 V and the opposite occurs when the sky view is 0%, approaching the maximum value (2.5 V). These results mean that decreasing sky view leads to increases in the output voltage until it approaches 2.5 V at 0% sky view (full shade).

5.2 Environment Testing

The ESJ has been used with an ambient 501 Biometer to estimate the erythemally effective UV exposure. Validation field trials and individual walking tests were undetaken where exposure estimates measured using the ESJ technique were validated against the output of a handheld PMA2100 radiometer. The roof-mounted biometer which was employed to measure ambient global UV was calibrated to the handheld PMA2100 to ensure the comparability of the results measured by the application of the ESJ.

A total of 5 individual walking tests or field trials were conducted. Each trial test was performed by holding a wooden board with the ESJ and PMA2100 attached to it while the researcher walked around and through different types of environment, including a variety of shade types, to show the ability of the ESJ to classify periods in shaded environments, periods in direct sun and periods indoors. Preliminary environmental test results showed that the ESJ is sensitive to the environment where the obtained voltage was 2.5 V when the ESJ was placed indoors, and 0 V when the ESJ was placed outdoors.

Environmental characterisation tests were important to show the ability of the ESJ to classify the type of environment typically occupied by users. The results obtained from these tests showed that the output voltage of the ESJ increased with increasing shade density (reduced sky view). The output voltage of the ESJ at each static environment reflected the type of shade in that environment. More specifically, in a full shaded environment, the ESJ output voltage was a straight line, consistently occurring at 2.5 V. The output voltage of the ESJ in partially shaded environments, including light and heavy tree shade, a shade structure and a verandah showed fluctuations in the signal voltage between 0 V and 2.5 V. However, in an open environment (no shade) the output voltage of the ESJ was consistently 0 V. The results presented here showed the ability of the ESJ to determine and classify (in terms of shade) the type of the environment where the users were located.

Results of individual walking tests confirmed the ability of the ESJ to detect an individual's sunlight exposure patterns. Based on the results obtained, the ESJ classified the type of the environment where individuals are present. More specifically, the ESJ detected the periods in direct sun and periods in shaded environments. Even the type of shade was detected by the ESJ, which was able to distinguish between indoor shade or tree shade. In addition to that, the type of tree shade was detected, that is, whether it was likely to be heavy or light tree shade.

The developed ESJ in this project could be used to determine when a subject was outside, but a UV dosimeter cannot do that. A UV dosimeter measures the integrated exposure to a defined waveband, typically the short wavelength UVB which is responsible for the human erythema response in fair skinned individuals.

By utilising the abundant IR in outdoor sunlight (which is several orders of magnitude higher than naturally available UVB in the solar spectrum), the ESJ can provide an accurate record of

outdoor exposure timing without the need for individual instrument calibration and amplification electronics.

The ESJ applied in this research was also shown to be sensitive to changing shade condition (see section 3.4 and Figure 3-10). It has recently been noted in field trials, that electronic UV dosimeters are less sensitive to changing shade conditions compared against portable UVR instruments, such as the PMA2100 (solar light co. PA USA) which was utilised in this project (Dobbinson et al. 2016). Furthermore, electronic UV dosimeters sold commercially to researchers, including the commercially available Scienterra and other AlGaN variants (Allen & McKenzie 2010, Liley et al. 2010) must be individually calibrated to the environment in which they are intended to be used. This involves exposing the electronic UV dosimeter for the necessary period of exposure likely to be incurred by study participants and must be performed in the same location of the study because the rate of UV energy received per unit time changes significantly depending on time of day and latitude. Customised calibration of electronic UV dosimeters increases the cost of these products compared to the ESJ which can be manufactured from readily available parts listed in Chapter 2.

This project provides a straightforward methodology that can be adapted by research teams interested in monitoring individual exposure patterns to sunlight. Therefore, the ESJ as proposed has the potential to provide proxy estimates of personal exposure to solar UVB and UVA –both solar spectra that are linked to skin cancer, ageing and other diseases (Chapter 1); as well as visible blue light exposure – linked potentially with age-related macular degeneration in human populations (Taylor et al. 1990) provided ambient measures of these solar wavebands are available in proximity to the user. Furthermore, monitoring of the IR waveband may also prove beneficial to future research teams given IR solar radiation may itself be deleterious to human skin tissue (Barolet et al. 2016).

The ESJ provided details of behavioural exposure patterns, not able to be recorded to such high resolution using traditional self-reported sun diaries. High sampling rates improve the accuracy of long-term epidemiological cumulative exposure studies. This, and the erythemally effective UV exposure estimates derived using the ESJ technique, showed that personal solar UV exposure estimates could be approximated, making the ESJ a potentially useful tool that can be utilised in future solar radiation studies.

References

AAP (American Academy of Pediatrics) 2011, 'Policy Statement-Ultraviolet Radiation: A Hazards to Children and Adolescents', *Pediatrics*, vol. 127, no.3, pp. 588-597. Available at: http://pediatrics.aappublications.org/content/pediatrics/early/2011/02/28/peds.2010-3501.full.pdf.

Allen, MW & Mckenzie, RL 2010, 'Electronic UV dosimeters for research and education', Proceedings of the NIWA UV Workshop, Queenstown, 7-9 April, Paper 11.

Amar, A 2014,'Development and characterisation of an ultra-long exposure UV dosimeter', PHD Thesis, University of Southern Queensland, Australia.

Amar, A & Parisi, AV 2012, 'investigation of unstabilized polyvinyl chloride (PVC) for use as a long-term UV dosimeter: Preliminary results', *Measurement Science and Technology*, vol. 23, no. 8, pp. 1-7.

Amar, A & Parisi, AV 2013, 'Spectral response of solvent-cast polyvinyl chloride (PVC) thin film used as long -term UV dosimeter', Journal of photochemistry and photobiology, vol. 125, pp. 115-120.

Ambas, V & Baltas, E 2014, 'Spectral Analysis of Hourly Solar Radiation', Springer International Publishing, vol. 1, no. 3, pp. 251-263.

Aphalo, PJ, Albert, A, Olof Bjorn, L, McLeod, A, Robson, TM, Rosenqvist 2012, 'Beyond the Visible: A Handbook of Best Practice in plant UV photobiology', COST Action FA0906 UV4growth. Helsinki: University of Helsinki, Division of Plant Biology. ISBN 978-952-10-8362-4 (Paperback), 978-952-10-8363-1 (PDF).

Ascherio, A., Munger, K.L., Simon, K.C. 2010. 'Vitamin D and multiple sclerosis', *The Lancet: Neurology*, vol. 9, no. 6, pp. 599-612.

Australian Bureau of Statistics (ABS), 2014. 3303.0 – Causes of Death, Australia, 2012. Canberra. Available at: http://www.abs.gov.au/AUSSTATS/abs@.nsf/allprimarymainfeatures/47E19CA15036B04BCA2577570014668B?opendocument.

Bais, AF, Mckenzie, RL, Bernhard, G, Aucamp, PJ, Ilyas, M, Madronich, S & Tourpalia, K 2015, 'Ozone depletion and climate change: impacts on UV radiation', *Photochemical & Photobiological Sciences*, vol. 14, pp. 19-52.

Barolet, D. Christiaens, F., Hamblin, M.R. 2016, 'Infrared and skin: Friend or foe', *Journal of Photochemistry and Photobiology B: Biology*, vol. 78, pp. 78-85.

Caldwell, MM, Gold, WG, Harris, G & Ashurst, CW 1983, 'A modulated lamp system for solar UV-B (280-320 nm) supplemental studies in the field', Photochemistry and photobiology, vol. 37, no.3, pp. 479-485.

CCA (Cancer Council Australia) 2015 a, 'Skin Cancer', Available at: http://www.cancer.org.au/about-cancer/types-of-cancer/skin-cancer.html . Accessed 1 November 2015.

CCA (Cancer Council Australia) 2015b, Skin Cancer Statistics & Issues, Available at: http://wiki.cancer.org.au/skincancerstats/Skin_Cancer_Statistics_and_Issues. Accessed 3 November, 2015.

CCA (Cancer Council Australia) 2015a, Skin cancer incidence and mortality, Available at: http://wiki.cancer.org.au/skincancerstats_mw/index.php?title=Skin_cancer_incidence_and_mortality&oldid=554 ., Accessed: 11 November 2015.

CCA (Cancer Council Australia) 2016, Skin Cancer Statistic & Issues : Skin cancer incidence and mortality, Available at: https://wiki.cancer.org.au/skincancerstats/Skin_cancer_incidence_and_mortality , Accessed 3/9/2018.

CCA (Cancer Council Australia) & ACD (The Australian College of Dermatologists 2009, 'Skin cancer prevention: A blue chip investment in health. Chair, National Skin Cancer Committe. https://www.cancer.org.au/content/pdf/CancerControlPolicy/Publications/MediaMaterials/Skin_Cancer_Prevention-a_Blue_Chip_Investment.pdf

Cancillo, ML, Serrano, A, Anton, M, Garcia, JA, Vilaplana, JA & Cachoro, VE 2005, 'Calibration method for broadband ultraviolet radiometers: Improving solar zenith angle dependence', Manuel Anton.

Casale, G, Siani, AM & Colosimo, A 2009, 'Polysulphone dosimetry: a tool for personal exposure studies', Biophysics and Bioengineering Letters, vol. 2, no. 1, pp. 1-14.

Chapman, S 1930, 'A theory of upper atmospheric ozone', *Memoirs of the Royal Meteorological society*, vol. 3, pp. 103-25.

Chodick, G, Kleinerman, RA, Linet, MS, Fears, T, Kwok, RK, KImlin, MG, Alexander, BH & Freedman, DM 2008, 'Agreement Between Diary Records of Time Spent Outdoors and Personal

Ultraviolet Radiation Dose Measurements', *Photochemistry and Photobiology*, vol. 84, no.3, PP. 713-718.

CIE (International Commission on Illumination) 1987, 'A reference action spectrum for ultraviolet induced erythema in human skin, 'CIE-Journal, vol. 5, no. 1, pp. 17-22.

CIE 1993, 'CIE Publication No. 98-1992: Personal dosimetry of UV radiation', Color Research & Application, vol. 18, no. 3, pp. 226-7.

CIE 1998, Erythema reference action spectrum and standard erythema dose, CIE 007/E-1998, Commission Internationale de l'Eclairage, Vienna.

Coohill, TP 1989, 'Ultraviolet action spectra (280 to 320 nm) and solar effectiveness spectra for high plants', Photochemistry and photobiology, vol. 50, no. 4, pp. 451-457.

Dahlback, A 2008, 'Global monitoring of atmospheric ozone and solar UV radiation', *Solar Radiation and Human Health*, Oslo: The Norwegian Academy of Science and Letters. pp. 23-34.

Damian, DL, Mathews, YJ, Phan, TA & Halliday, GM 2011, 'An action spectrum for ultraviolet radiation- induced immunosuppression in humans', *British Association of Dermatologists*, vol. 164, no. 3, pp. 657-659.

De Gruijl, FR, 2000, 'Health effects from the sun's ultraviolet radiation and ozone as a stratospheric sunscreen', Global change & Human health, vol. 1, no. 1, pp. 26-40.

Deluisi, J, Theisen, D, Augustine, J, Disterhoft, P, Lantz, K, Weatherhead, E, Hodges, G Cornwall, C, Petropavlovskikh, I, Stevermer, A, Wellman, D & Barnett, J 2003, 'On the correspondence between surface UV observations and TOMS determinations of surface UV: a potential method for quality evaluating world surface UV observtions', Annals of Geophysics, vol. 46, N. 2, pp. 295-308.

Di Menno, I, Moriconi, ML, Di Menno, M, Casale, GR & Siani, AM 2002, 'Spectral Ultraviolet Measurements by a Multichannel Monitor and Brewer Spectroradiometers: A Field Study Radiation Protection Dosimetry, vol. 102, no. 3, pp. 259-263.

Diffey, BL, Davis, A, Johnson, M, & Harrington, TR 1977, 'A dosimeter for long wave ultraviolet radiation', *British Journal of Dermatology*, vol. 97, no. 2, pp. 127-130.

Diffey, BL 1984, 'Personal ultraviolet dosimetry with Polysulphone film badges', *Photodermatol*, vol. 1, no. 3, pp. 151-157.

Diffey, BL 1991,' Solar Ultraviolet radiation effects on biological system', *Review in Physics in Medicine and Biology*, vol. 36, no.3, pp. 299-328.

Diffey, BL 1998, 'Ultraviolet Radiation and Human Health', *Clinical Dermatology,* vol. 16, no. 1, pp. 83-89.

Diffey, BL 2002, 'Source and measurements of ultraviolet radiation', *Methods*, vol. 28, pp. 4-13.

Dobbinson, S., Niven, P., Buller, D., Allen, M., Gies, P. & Warne, C. 2016, 'Comparing handheld meters and electronic dosimeters measuring UV levels under shade and in the Sun', *Photochemistry & Photobiology*, vol. 92, pp. 208-214.

Downs, N, Parisi, AV, McDonnell, B & Thornton, P 2008, 'Measurement variation and factors influencing the UV index', *Teaching Science*, vol. 54, no. 2, pp. 8-13.

Downs, N, Schouten, P, Parisi, A & Turner, J 2009, 'Measurement of the upper body ultraviolet exposure to golfers: nonmelanoma skin cancer risk and the potential benefits of exposure to sunlight', Photodermatology, Photodermatology and Photomedicine, vol. 25, no. 6, pp. 317-324.

Downs, N, Parisi, AV, Galligan, L, Turner, J, Amar, A, King, R, Ultra, F & Butler, H 2016, 'Solar radiation and the UV index: An application of numerical integration, trigonometric functions, online education and the modelling process', *International Journal of Research in Education and Science (IJRES),* vol. 2, no. 1, pp. 179-189.

Envall, J, ylianttila, L, Moseley, H, Coleman, A, Durak, M, Karha, P & Ikonen, E 2006, 'Investigation of comparison methods for UVA Irradiance responsivity calibration facilities', *Metrologia,* vol. 43, no. 2, https://doi.org/10.1088/0026-1394/43/2/S06

Geiss, O, Grobner, J & Rembges D 2003,'Manual for Polysulphone Dosimeters: Characterisation, Handling and Application as personal UV Exposure Devices', Physical & chemical Exposure (PEC), EUR 20981 EN.

Grant, WB 2007, 'Roles of solar UV radiation and vitamin D in human health and how to obtain vitamin D', *Exper Rev*, *Dermatol*, no. 2, pp. 563- 577

Green, A, Siskind, V, Hansen, ME, Hanson, L, & Leech, P 1989, 'Melanocytic nevi in school children in Queensland', *Journal of the American Academy of Dermatology*, vol. 20, pp. 1054-1060.

Greinert, R, De Vries, E, Erdmann, F, Espina, C, Auvinen, A, Kesminiene, A & Schuz, J 2015, 'European Code against Cancer 4th edition: ultraviolet radiation and cancer', *Cancer Epidemiology*, DOI: 10.1016/j.canep.2014.12.014.

Harrison, GI & Young, AR 2002, 'Ultraviolet radiation-induced erythema in human skin', *Methods,* vol. 28, pp. 14-19.

Honigsmann, H 2002, 'Erythema and pigmentation', *Photodermatology, photoimmunology & Photomedicine*, vol. 18, no. 2, pp. 75-81.

Horneck, G, Quintern, LE, Tetterg, P, Eschweiler, U & Gorgen, E 1993,'Biologic Effects of light 1993, ed. EG, Jung and MF, Holick pp. 501-506, Walter de Gruyter.

Huber, M, Blumthaler, M & Schreder, J 2003, 'Solar UV measurements with Robertson-Berger type instruments: Influence of the detector's internal humidity status', Agric. For. Meteorol, vol. 120, pp. 39-43. doi:10.1016/j.agrformet.2003.08.010.

Hussein, MR 2005, 'Ultraviolet radiation and skin cancer: molecular mechanisms', *Journal of Cutaneous Pathology,* vol. 32, pp. 191-205.

International Agency for Research on Cancer (IARC), 2012, 'Solar and ultraviolet radiation, IRAC Monographs, vol. 100D, pp. 35-101, Available at: http://monographs.iarc.fr/ENG/Monographs/vol100D/mono100D-6.pdf. Accessed: 25/9/2015.

Jaggernath, J, Haslam, D & Naidool, KS 2013, 'Climate change: Impact of increased ultraviolet radiation and water changes on eye health', *Health*, vol. 5, no. 5, pp. 921-930.

Juzeniene, A & Moan, J 2012, 'Beneficial effects of UV radiation other than via vitamin D production', *Dermato-Endocrinology*, vol. 4, no. 2, pp. 109-117.

Kerr, JB, 2005,'Understanding the factors that affect surface ultraviolet radiation', *Optical engineering*, vol. 44, no. 4, pp. 1-9.

Kerr, JB & Fioletov, VE 2008, 'Surface Ultraviolet Radiation', *Atmosphere-Ocean*, vol. 46, no. 1, pp.159-184.

Kikas, U, Reinart, A, Vaht, M & Veismann, U 2001, 'A case study of the impact of boundary layer aerosol size distribution on the surface UV irradiance', *Atmospheric Environment*, vol. 35, pp.5041-5051.

Knuschke, P & Barth, J 1996, 'Biological weighted UV dosimetry', Photochemistry and Photobiology, vol. 36, pp. 77-83.

Koster, B, Sondergaard, J, Nielsen, JB, Allen, M, Bjerregaard, M, Olsen, A & Bentzen, J 2015,'Feasibility of smartphone diaries and personal dosimeters to quantitatively study exposure to ultraviolet radiation in small national sample', *Photodermatology, Photoimmunology & Photomrdicine*, vol. 31, no.5, pp. 252-260.

Leiter, U & Garbe, C 2008, 'Epidemiology of Melanoma and Nonmelanoma Skin Cancer- The Role of Sun light', *Advances in Experimental Medicine and Biology*, vol. 624, pp. 89-103. DOI: 10.1007/978-0-387-77574-6_8.

Leszczynski, K 2002, 'Advances in traceability of solar ultraviolet radiation measurements', STUK-A189, Helsinki, Fin-land: STUK (Radiation and Nuclear Safety Authority). Available at: https://helda.helsinki.fi/bitstream/handle/10138/23142/advances.pdf?sequence=2.

Liley, B, Liley, J, Allen, M, Robinson, J, Mckenzie, R & the UV- vitamin D team 2010, 'Personal exposures to UV radiation in New Zealand', Proceedings of the UV conference, 'UV radiation and its effects-an update 2010', Queenstown, New Zealand, PP. 29-30.

Lucas, RM & Ponsonby, AL 2002, Ultraviolet radiation and health: friend and foe', *Medical Journal of Australia*. Vol. 177, pp. 594-598.

Lysko, MD 2006, 'Measurement and Models of solar irradiance', PHD thesis, Norwegian University of Science and technology, Faculty of Natural Science and Technology, Department of Physics. Available at: http://www.academia.edu/2032709/Measurement_and_Models_of_Solar_Irradiance.

Madronich, S, Mckenzie, RL, Bjorn, LO & Caldwell, MM 1998,'Changes in biologically active Ultraviolet radiation reaching the Earth's surface', *Journal of photochemistry and photobiology B: Biology*, vol. 46, pp. 5-19.

Majdi, M, Milani, BY, Movahedan, A, Wasielewski, L, Djalilian, AR, 2014, 'The Role of Ultraviolet Radiation in Ocular System of Mammals', Photonics, vol. 1, pp. 347-368. doi: 10.3390/photonics1040347.

McKinlay, AF & Diffey, BL. 1987, "A Reference Action Spectrum for Ultraviolet Induced Erythema in Human Skin", CIE Journal, vol. 6, pp. 17-22.

Melanoma Institute Australia 2018: Melanoma facts and statistics, Available at: https://www.melanoma.org.au/understanding-melanoma/melanoma-facts-and-statistics/. Accessed 15/9 2018.

Model 501 UV Biometer Manual 2006, 'Manual of 501 UV biometer', Solar Light Company. https://solarlight.com/wp-content/uploads/2013/02/501.pdf

Nan-bin, X, 2014, 'Evolutionary Characteristics of Total Solar Irradiance', Chines Astronomy and Astrophysics, vol. 38, no. 1, pp. 75-84.

Narayanan, DL, Saladi, RN & Fox, JL, 2010, 'Ultraviolet Radiation and skin cancer', *International Journal of Dermatology*, vol. 49, no. 9, pp. 978-986.

Nozawa, H, Yamamoto, H, Makita, K, Schuch, NJ,Pinheiro, DK, Carbone, S, Mac-Mahon, RM & Foppiano, AJ 2007, 'Ground-based observation of solar UV radiation in Japan, Brazil and Chile', *Revista Brasileira de Geofisica*, vol. 25, no. 2, pp. 17-25. https://dx.doi.org/10.1590/S0102-261X2007000600003

Olds, WJ 2010, 'Elucidating the Links Between UV Radiation and Vitamin D Synthesis: Using an *In Vitro* Model', PHD thesis, Queensland university of Technology, Available at: http://eprints.qut.edu.au/32073/1/William_Olds_Thesis.pdf., Accessed: 3/1/2016.

O'Riordan, DL, Glanz, K, Gies, P & Elliott, T 2008, 'A pilot Study of the Validity of Self- Reported Ultraviolet Radiation Exposure and Sun Protection Practices Among Lifeguards, Parents and Children', Photochemistry and Photobiology, vol. 84, pp. 774-778. DOI: 10.1111/j.1751-1097.2007.00262.x.

Osteoporosis Australia Medical & Scientific Advisory Committe 2014, Vitamin D Factsheet: A vitamin D statement from our Medical Committee. https://www.osteoporosis.org.au/vitamin-d

Parisi, Av, Green, A & Kimlin, MG 2001, 'Diffuse solar ultraviolet radiation and implications for preventing human eye damage', *Photochemistry and photobiology*, vol. 73, no. 2, pp. 135-139.

Parisi, AV 2004, 'Solar UV radiation measurements with polysulphone', chemistry in Australia, vol. 71, no. 2, pp. 16-8.

Parisi, AV, Sabburg, J & Kimlin, MG 2004, 'Scattered and Filtered Solar UV Measurements', vol. 17, Advances in Global Change Research, Kluwer Academic press, Dordrecht, The Netherlands.

Parisi, AV 2005, 'Physics concepts of solar ultraviolet radiation by distance education', *European Journal of physics*, vol. 26, no. 2, pp. 313-320.

Parisi, A & Kimlin, MG 2003, 'Extending the dynamic range of polysulphone for measuring UV exposures. In: SPIE Annual Meeting, San Diego, CA, USA.

Parisi, AV & Kimlin, MG 2005 a, 'Solar UVA exposures', *In: Optics & Photonics,* San Diego, CA, USA.

Parisi, AV & Kimlin, MG 2005 b, 'Thin film dosimeter for the assessment of UVA exposures to humans. In: 30th Annual conference of the Australian Radiation Protection Society Conference (ARPS 2005), 13-16 November 2005, Melbourne, Australia.

Parisi, AV & Turnbull, DJ 2005, 'Diffuse solar ultraviolet radiation', *International Ophthalmology Clinics*, vol. 45, no. 1, pp. 19-27.

Parisi, AV, Sabburg, J, Turner, J & Dunn, PK 2008, 'Cloud observations for statistical evaluation of the UV index at Toowoomba, Australia', *International Journal of Biometeorology*, vol. 52, no. 3, pp.159-166.

PS (Position Statement) 2006, Estimates of Beneficial and harmful sun exposure times during the year for major Australian population centres, *Med. J. Aust.*, vol. 184, pp. 338-341.

Rajakumar, K, Greenspan, SL, Thomas, SB & Holick, MF, 2007, 'Solar Ultraviolet Radiation And Vitamin D', American Journal of public Health, vol. 97, no. 10, pp. 1746-1754.

Sabburg, J & Wong, J 2000, 'The effect of clouds on enhancing UVB irradiance at the Earth's surface: A one-year study', *Geophysical research letters*, vol. 27, no. 20, pp. 3337-3340.

Sabburg, J, Parisi, AV & Kimlin, MJ 2003,'Enhanced spectral UV irradiance: a one-year preliminary study, *Atmospheric research*, vol. 66, pp. 261-272.

Schouten, PW, Parisi, AV & Turnbull, DJ 2010, 'Usage of the polyphenylene oxide dosimeter to measure annual solar erythemal exposures', *Photochemistry and Photobiology*, vol.86, no.3, pp. 706-10.

Schwarz, T 2005, 'Mechanisms of UV-induced immunosuppression', *The Keio Journal of Medicine,* vol. 54, no. 4, pp. 165-171.

Scienterra Limited 2019, UV dosimeter, available at: http://www.scienterra.com/home/4567276438/uv-dosimeter/3113961, Accessed 6 August 2019.

Seckmeyer, G, Klingebiel, M, Riechelmenn, S, Lohse, I, Mckenzie, RL, Liley, JB, Allen, MW, Siani, AM & Casale, GR 2012, 'A critical assessment of two types of Personal UV dosimeters', *Photochemistry and Photobiology*, vol. 88, no. 1, pp. 215-22.

Seidlitz, HK & Krins, A 2006, 'Solar radiation and its measurment', in Ghtti, F, Checcucci, g & Bornman, JF (eds), environmental UV radiation: Impact on ecosystems and human Health and predictive models, Springer, Dordrecht, The Netherlands, vol. 57, pp. 25-38.

Serrano, MA, Canada, J, Moreno, JC, Gurrea, G, Members of the Valencia solar Radiation Research Group 2014. 'Occupational UV exposure of environmental agents in Valencia, Spain', *Photochem Photobiol*, vol. 90, no. 4, pp. 911-8.

Sherman, Z. 2014, 'Developments in electronic UV dosimeters', NIWA UV Workshop, Auckland, 15-17 April, 2014.

Sivamani, RK, Crane, LA & Dellavalle, RP 2009, 'The Benefits and risks of ultraviolet tanning and its alternatives: the role of prudent sun exposure', *Dermatologic clinics*, vol. 27, no. 2, pp. 149-54.

Solanki, SK, Krivova, NA & Haigh, JD 2013, 'Solar Irradiance Variability and Climate', *Annual Review of Astronomy and Astrophysics*, vol. 51, no. 1, PP. 331-351.

Solar Light Co n.d., 'A comparison of Spectroradiometers to Radiometers for UV Radiation Measurements', Solar Light CO., Inc. 100 East Glenside Avenue, Glenside, PA 19038. https://solarlight.com/wp-content/uploads/2013/04/spectro.pdf

Stamnes, K & Stamnes, JJ 2008, 'Transport of Solar Radiation through the Atmosphere: Aspects Relevant for Health, in E. Bjertness (ed.), Solar Radiation and Human Health, The Norwegian Academy of Science and Letters, Oslo, pp. 9-22.

Taylor, H.R., Munoz, B., West, S., Bressler, N.M., Bressler, S.B. & Rosenthal, F.S. 1990, 'Visible light and risk of age-related macular degeneration', *Transactions of the American Opthalmological Society*, vol. 88, pp. 163-178.

Thieden, E, Philipsen, PA, Sandby-Moller, J, Heydenreich, J & Wulf, HC 2004, 'Proportion of Lifetime UV Dose Received by children, Teenagers and Adults Based on Time-Stamped Personal Dosimetry', *The Journal of Investigative Dermatology*, vol. 123, no. 6, pp. 1147-1150.

Turnbull, D 2005, 'Development of an Improved Shade Environment for Reduction of personal UV Exposure', PHD Thesis, University of Southern Queensland, Australia.

Turnbull, D & Parisi, A 2010, 'Vitamin D irradiance in summer shade and sun', *Household and Personal Care Today*, vol. 3, pp. 4-6. ISSN 2035-4614.

Turner, J & Parisi, AV 2009, 'Measuring the influence of UV reflection from vertical metal surfaces on humans', Photochemical and Photobiological Sciences, vol. 8, no. 1, pp. 62-69.

Van der Gaad & Brehoff, L 2014, 'Effects of food and vitamin D supplements on serum 25(OHD)3 concentration in children during winter months', *Food*, no. 3, pp. 632-41. doi:10.3390/foods3040632.

Wainwrigth, L 2012, 'Characterisation and evaluation of a miniaturised polyphenylene oxide dosimeter", PHD thesis, University of Southern Queensland, Australia.

Wainwrigth, L, Parisi, AV, Downs, N 2016, 'Dual calibrated dosimeter for simultaneous measurements of erythemal and vitamin D effective solar ultraviolet radiation', Photochemistry and photobiology, B, Biology, vol.157, pp. 15-21. Doi: 10.1016/j.jphotobiol.

Wang, F, Hu, L, Gao, Q, Gao, Y, Liu, G, Zheng, Y & Liu, Y 2014, 'Risk of Ocular Exposure to Biologically Effective UV Radiation in Different Geographical Directions', *Photochemical and Photobiology*, vol. 90, no. 5, pp. 1174-1183.

Webb, AR 1998, 'UVB Instrumentation and Applications', *Gordon and Breach Science Publication*, Amsterdam.

Whiteman, D & Neale, R 2004, 'The role of genetics in the prevention of skin cancer. In Hill, DJ, Elwood, M & English, DR, editors, *Prevention of Skin Cancer*, vol. 3 of Cancer Prevention- Cancer Causes, Chapter 7, pp. 117-140. Kluwer Academic Publisher. The Netherlands.

WHO (World Health Organization) 1994, Environmental health criteria 160: Ultraviolet radiation, World Health Organization, Geneva. http://www.inchem.org/documents/ehc/ehc/ehc160.htm#SubSectionNumber:3.1.1.

WHO (World Health Organization) 2002, Global Solar UV Index: A Practical Guide, http://www.who.int/uv/publications/en/UVIGuide.pdf

WHO (World Health Organization) 2018, Ultraviolet Radiation: UV Index, http://www.who.int/uv/intersunprogramme/activities/uv_index/en/index4.html

Whright, CY, Albers, PN, Mathee, A, Kunene, Z, D'Este, C, Swaminathan, A & Lucas, RM 2017, Sun protection to improve vaccine effectiveness in children in high ambient ultraviolet radiation and rural environment: an intervention study. BMC public health, vol. 17, no. 1. doi:10.1186/s12889-016-3966-0.

Wong, JCF & Parisi, AV 1999, 'Assessment of ultraviolet radiation exposures in photobiological experiments', in Protection against the hazards of UVR Internet Conference.

Woods, TN, Rottman, GJ, Harder, JW, Fontenla, J, Kopp, G, Lawrence, GM, Lean, J, McClintock, WE, Pilewskie, P, Richard, E, Snow, M, Whote, OR, Wu, DL, Cahalan, RF, Knapp, B, Kohnert, R, Lindholm, D, McCabe, D, Pankratz, C, Ryan, S & Vanier, B 2015, 'SRCE (Solar Radiation and Climate Experiment), University of Colorado, Laboratory for Atmospheric and Space Physics'. Available at: http://lasp.colorado.edu/home/sorce/data/, Accessed: 15/10/2015.

Wright, GY & Griffith, D 2015, 'Solar UVR instrument inter-comparison focusing on measurement interval recording setting and solar zenith angle as important factors', South African Society for Atmospheric Sciences 31st annual conference: Applying the weather, Hennops Revier Valley, South Africa

Yam, JC. & Kwok, AK. 2014, 'Ultraviolet light and ocular diseases', *Int Ophthalmol*, vol. 34, no. 2, pp. 383-400.

Young, AR 2006, 'Acute effects of UVR on human eyes and skin', *Progress in Biophysics and Molecular Biology,* vol. 92, no. 1, pp. 80-85.